arXiv:2205.07715v3 [hep-ex] 29 Nov 2022

Snowmass White Paper: Prospects of CP-violation measurements with the Higgs boson at future experiments

Editor: Andrei V. Gritsan,[1] Contributors: Henning Bahl,[2] Rahool Kumar Barman,[3] Ivanka Božović-Jelisavčić,[4] Jeffrey Davis,[1] Wouter Dekens,[5] Yanyan Gao,[6] Dorival Gonçalves,[3] Lucas S. Mandacarú Guerra,[1] Daniel Jeans,[7] Kyoungchul Kong,[8] Savvas Kyriacou,[1] Kirtimaan Mohan,[9] Ren-Qi Pan,[10] Jeffrey Roskes,[1] Nhan V. Tran,[11] Natasa Vukašinović,[4] and Meng Xiao[10]

[1]*Department of Physics and Astronomy, Johns Hopkins University, Baltimore, MD 21218, USA*
[2]*University of Chicago, Department of Physics, 5720 South Ellis Avenue, Chicago, IL 60637 USA*
[3]*Department of Physics, Oklahoma State University, Stillwater, OK, 74078, USA*
[4]*"VINČA" Institute of Nuclear Sciences, University of Belgrade, Belgrade, Serbia*
[5]*Institute for Nuclear Theory, University of Washington, Seattle WA 91195-1550, USA*
[6]*School of Physics and Astronomy, University of Edinburgh, Edinburgh, EH9 1ES, UK*
[7]*Institute of Particle and Nuclear Studies, KEK, 305-0801 Tsukuba, Japan*
[8]*Department of Physics and Astronomy, University of Kansas, Lawrence, Kansas 66045, USA*
[9]*Department of Physics and Astronomy, Michigan State University, East Lansing, MI 48824, USA*
[10]*Zhejiang Institute of Modern Physics, Department of Physics, Zhejiang University, Hangzhou, 310027, P. R. China*
[11]*Fermi National Accelerator Laboratory (FNAL), Batavia, IL 60510, USA*

(Dated: May 16, 2022)

The search for CP violation in interactions of the Higgs boson with either fermions or bosons provides attractive reference measurements in the Particle Physics Community Planning Exercise (a.k.a. "Snowmass"). Benchmark measurements of CP violation provide a limited and well-defined set of parameters that could be tested at the proton, electron-positron, photon, and muon colliders, and compared to those achieved through study of virtual effects in electric dipole moment measurements. We review the current status of these CP-sensitive studies and provide projections to future measurements.

Contents

I. Introduction 3

II. Framework of the Higgs CP study for Snowmass 3

III. Prospects of Higgs CP measurements at a photon collider 5

IV. Prospects of Higgs CP measurements at a muon collider 6
A. Muon collider at the H boson pole 6
B. High-energy muon collider 6

V. Prospects of Higgs CP measurements at a hadron collider 7
A. Gluon fusion process at a hadron collider 7
B. The $H\gamma\gamma$ and $HZ\gamma$ couplings at a hadron collider 7
C. The HZZ and HWW couplings at a hadron collider 9
D. The $Ht\bar{t}$ coupling at a hadron collider 9
E. The $H \to \tau^+\tau^-$ process at a hadron collider 11

VI. Prospects of Higgs CP measurements at an electron-positron collider 11
A. The VH process at an electron-positron collider 11
B. The VBF process at an electron-positron collider 12
C. The $t\bar{t}H$ process at an electron-positron collider 13
D. The $H \to \tau^+\tau^-$ and other decay processes at an electron-positron collider 13

VII. Prospects of Higgs CP measurements at a lepton-hadron collider 13
A. The VBF process at a lepton-hadron collider 13
B. The top-H process at a lepton-hadron collider 14

VIII. Comparison to EDM measurements 14

IX. Summary 15

A. Recent updates of the studies at a hadron collider 16

B. Recent updates of the studies at an electron-positron collider 17

C. EDM constraints 19

References 20

I. INTRODUCTION

The search for CP violation is an important research direction of future experiments in particle physics. CP violation is one of the requirements for baryogengesis [1]. So far the only experimental evidence for CP violation comes from quark flavor physics, which is consistent with the CKM mechanism appearing in the Standard Model (SM) of particle physics [2]. This SM mechanism is believed to be insufficient for generating the observed predominance of baryon matter over antimatter on a cosmological scale [3]. Therefore, the search for CP violation in interactions of the Higgs boson (H) with either fermions or bosons is an interesting path to search for a new mechanism.

Through the study of the HVV and $Hf\bar{f}$ tensor structure of interactions of the H boson with vector bosons (Z, W, γ, g) and fermions (t, τ), the CMS and ATLAS experiments on LHC have established that the J^{PC} quantum numbers of the H boson should be 0^{++}, if this boson has definite P and C [4–27]. This observation is consistent with the Standard Model (SM) expectation for these quantum numbers to be that of the vacuum. However, small violation of CP symmetry in those interactions cannot be excluded within the experimental precision of current measurements. Squeezing the allowed range of CP-violating parameters, or, alternatively, discovering non-zero CP violation in the H boson interactions, becomes an important target of experimental measurements [28–73].

Future high-energy physics experiments, either planned or proposed, have unique features for testing CP violation in the H boson interactions. For example, photon and muon colliders with a beam polarization scan could provide a unique opportunity to search for CP violation in couplings to either photons or muons. The electron-positron collider is positioned uniquely to search for CP violation in HVV interactions, with vector bosons appearing in electron-positron annihilation, and allow for CP studies in decay. Proton colliders provide an array of opportunities for HVV and $Hf\bar{f}$ studies in both production and decay, as already demonstrated by the LHC experiments.

This makes CP violation studies with the H boson an attractive reference measurement in the Particle Physics Community Planning Exercise (a.k.a. "Snowmass"), organized by the US High Energy Physics community to set directions in the field of particles physics for the next decade and beyond. Benchmark measurements of CP violation in interactions of the H boson with SM particles provide a limited and well-defined set of parameters that could be tested at future high-energy physics colliders. Moreover, these measurements can also be achieved through study of virtual effects in quark flavor physics and electric dipole moment (EDM) measurements. These CP violation effects are tiny in the SM, and they therefore become excellent null tests for comparing performance of future facilities. Beyond-the-SM (BSM) theories predict sizable CP violation effects, which could have profound implications for the future of particle physics, if discovered.

II. FRAMEWORK OF THE HIGGS CP STUDY FOR SNOWMASS

Since the discovery of the H boson by the ATLAS and CMS experiments on the Large Hadron Collider (LHC) [74, 75], the search for CP violation in its interactions started immediately [4–6]. The CP violation parameters were identified as benchmark measurements in the Snowmass-2013 Particle Physics Community Planning Exercise [76]. In that study, CP-violating parameters were defined in the coupling of the H boson to massive vector bosons (HVV), to massless vector bosons ($H\gamma\gamma$, $HZ\gamma$, Hgg), and to fermions ($Ht\bar{t}$, $H\tau\tau$, $H\mu\mu$). In this work, we build on that study, take advantage of both experimental and theoretical progress in the study of the H boson interactions over the past decade, and make assessment of prospects of the H boson CP study at the future facilities, both proposed and planned.

On the experimental front, measurements of CP violation parameters have been achieved on LHC experiments [4–24]. This allows us to make realistic quantitative projections to the HL-LHC. The main change on the theoretical front has been development of the Effective Field Theory (EFT) framework, and in particular SMEFT, where CP violation naturally appears from a sub-set of higher-dimension operators. Both developments have been discussed within the LHC Higgs and LHC EFT Working Groups [77, 78], where we rely on some of their efforts.

One could consider the study of CP violation to be redundant with respect to the larger project of EFT global fits. However, there are two reasons which make this consideration less reliable for the Snowmass studies. First of all, the global EFT fits are very complex with many parameters and assumptions invoked to reduce the number of those parameters. One of the common constraints applied in the current global EFT fits is the lack of CP-odd operators, effectively setting all CP violation effects to zero. Second, even when such CP constraints are not invoked, the actual measurements are often based on experimental information which is not necessarily truly CP-sensitive. This means that the measurement may be sensitive to the presence of the higher-dimension operators, but may not distinguish well between CP-odd and CP-even terms. Therefore, the idea of the dedicated CP-sensitive measurements of the H boson for the Snowmass studies is to provide simple but at the same time reliable benchmarks which could serve as a guide to compare future facilities.

As an example of the future measurement projections based on the global EFT fits, let us refer to the H boson studies performed for the 2020 European Strategy for Particle Physics Update [79]. In the EFT description of the H boson couplings, either 18 (with flavor universality) or 30 (with neutral diagonality) CP-even operators in the so-called Higgs basis were considered within the SMEFT framework, which invokes the SU(2)×U(1) EW symmetry. To assess the sensitivity to deviations from the SM in a basis-independent way the results of the fit were projected onto the following H boson effective couplings:

$$\mathrm{g}^{\mathrm{eff}\ 2}_{HX} \equiv \frac{\Gamma_{H\to X}}{\Gamma^{\mathrm{SM}}_{H\to X}}\,. \tag{1}$$

These parameters are convenient to compare different studies in a straightforward manner. However, these parameters do not allow for the CP structure in the HX interaction. Therefore, we expand this set of CP-conserving parameters with the following set, allowing for CP violation in each HX interaction:

$$f^{HX}_{CP} \equiv \frac{\Gamma^{CP\,\mathrm{odd}}_{H\to X}}{\Gamma^{CP\,\mathrm{odd}}_{H\to X} + \Gamma^{CP\,\mathrm{even}}_{H\to X}}\,, \tag{2}$$

where the partial decay $H \to X$ width is calculated with either the CP-odd or CP-even part of the amplitude. This definition is consistent with the CP-sensitive parameters f_{CP} defined for the Snowmass-2013 study [76]. These f_{CP} parameters have been adopted in the LHC measurements as well, for a recent summary refer to Ref. [20]. Therefore, we adopt Eq. (2) for the benchmark parameter measurements.

We note that Eq. (2) is defined in decay of the H boson. For example, the general scattering amplitude that describes the interaction of the H boson with the fermions, such as $\tau^+\tau^-$, $\mu^+\mu^-$, $b\bar{b}$, and $t\bar{t}$, can be written as

$$A(H \to f\bar{f}) = \frac{m_f}{v}\bar{u}_2\left(b_1^{Hf\bar{f}} + ib_2^{Hf\bar{f}}\gamma_5\right)u_1\,. \tag{3}$$

Therefore, the CP-sensitive parameter takes the form

$$f^{Hf\bar{f}}_{CP} \equiv \frac{|b_2^{Hf\bar{f}}|^2}{|b_1^{Hf\bar{f}}|^2 + |b_2^{Hf\bar{f}}|^2} = \sin^2\left(\alpha^{Hf\bar{f}}\right)\,. \tag{4}$$

Technically, Eq. (2) does not cover $Ht\bar{t}$ interactions, because the decay $H \to t\bar{t}$ is not possible. However, we expand the definition in Eq. (4) to all fermion couplings. The effective mixing angle $\alpha^{Hf\bar{f}}$, introduced in Eq. (4), is often used in describing the CP-odd amplitude contribution. However, we adopt a more general parameterization with effective cross-section fractions because they allow more than two amplitude contributions, as this becomes important in description of the HVV interactions, discussed below.

For the coupling to the gauge bosons, such as WW, ZZ, $Z\gamma$, $\gamma\gamma$, or gg, the scattering amplitude can be written as

$$A(H \to V_1V_2) = v^{-1}\left(a_1^{HVV}m_V^2\epsilon_1^*\epsilon_2^* + a_2^{HVV}f^{*(1)}_{\mu\nu}f^{*(2),\mu\nu} + a_3^{HVV}f^{*(1)}_{\mu\nu}\tilde{f}^{*(2),\mu\nu}\right)\,, \tag{5}$$

where a_i^{HVV} are generally q^2-dependent coefficients scaling the three unique Lorentz structures, described with the help of the (conjugate) field strength tensor $f^{(i),\mu\nu}$ ($\tilde{f}^{(i),\mu\nu}$) of a gauge boson with momentum q_i and polarization vector ϵ_i. In the following, we will keep only the first-order q^2-expansion of Eq. (5) with constant coefficients a_i, which correspond to dimension-six operators in the effective Lagrangian formulation. The presence of the CP-odd contribution a_3^{HVV}, which can be treated as constant in this expansion, indicates CP violation, and the CP-sensitive parameter takes the form

$$f^{HVV}_{CP} = \frac{|a_3^{HVV}|^2}{\sum|a_i^{HVV}|^2(\sigma_i^{HVV}/\sigma_3^{HVV})}\,, \tag{6}$$

where σ_i is the effective cross-section of the $H \to VV$ decay process corresponding to $a_i = 1, a_{j\neq i} = 0$.

This brings us to the summary of possible CP-sensitive measurements in the H boson interactions in Table I. In the following, we will review unique features of photon, muon, hadron, and electron-positron colliders, where we keep the energy and luminosity scenarios the same as in the Snowmass-2013 studies [76] for easy comparison and because several projections (such as CP violation in fermion couplings) have not been updated. More recent projections for electron-positron colliders have been shown with higher luminosity, and we indicate in Appendix B how expectations scale to an order of magnitude higher luminosity for some of the couplings. These higher luminosity collider scenarios are consistent within a factor of two with the more recent recommendations for Snowmass-2022 studies, as outlined in Ref. [80].

TABLE I: List of expected precision (at 68% C.L.) of CP-sensitive measurements of the parameters f_{CP}^{HX} defined in Eq. (2). Numerical values are given where reliable estimates are provided, ✓ mark indicates that feasibility of such a measurement could be considered. The $e^+e^- \to ZH$ projections are performed with $Z \to \ell\ell$ in Appendix B but scaled to a ten times larger luminosity to account for $Z \to q\bar{q}$.

Collider	pp	pp	pp	e^+e^-	e^+e^-	e^+e^-	e^+e^-	e^-p	$\gamma\gamma$	$\mu^+\mu^-$	$\mu^+\mu^-$	target
E (GeV)	14,000	14,000	100,000	250	350	500	1,000	1,300	125	125	3,000	(theory)
$\mathcal{L}$ (fb^{-1})	300	3,000	30,000	250	350	500	1,000	1,000	250	20	1,000	
HZZ/HWW	$4.0{\cdot}10^{-5}$	$2.5{\cdot}10^{-6}$	✓	$3.9{\cdot}10^{-5}$	$2.9{\cdot}10^{-5}$	$1.3{\cdot}10^{-5}$	$3.0{\cdot}10^{-6}$	✓	✓	✓	✓	$< 10^{-5}$
$H\gamma\gamma$	–	0.50	✓	–	–	–	–	–	0.06	–	–	$< 10^{-2}$
$HZ\gamma$	–	$\sim$1	✓	–	–	–	$\sim$1	–	–	–	–	$< 10^{-2}$
Hgg	0.12	0.011	✓	–	–	–	–	–	–	–	–	$< 10^{-2}$
$Ht\bar{t}$	0.24	0.05	✓	–	–	0.29	0.08	✓	–	–	✓	$< 10^{-2}$
$H\tau\tau$	0.07	0.008	✓	0.01	0.01	0.02	0.06	–	✓	✓	✓	$< 10^{-2}$
$H\mu\mu$	–	–	–	–	–	–	–	–	–	✓	–	$< 10^{-2}$

III. PROSPECTS OF HIGGS CP MEASUREMENTS AT A PHOTON COLLIDER

The photon collider has a unique feature in that it can be used to study the H boson couplings to photons in direct production $\gamma\gamma \to H$. It is also possible to study the H boson couplings in decay, such as CP structure in $H \to \tau^+\tau^-$ or $H \to 4f$. However, the decay measurements critically depend on the number of produced H bosons, and a Higgs factory in either lepton or proton collisions is better positioned to make those measurements. In this Section, therefore, we focus on the $H\gamma\gamma$ measurements, which are unique to the photon collider.

The coupling of the H boson to two photons cannot happen at tree level, but can be generated by loops of any charged particles. In the SM, those are the charged fermions and W boson. In the SM, CP violation is tiny, as it can be generated only at three-loop level. In BSM theories, new heavy states can contribute to the loop, and could generate sizable CP violation. Alternatively, CP violation in the H boson couplings to SM particles could also generate CP-odd contributions to the $H\gamma\gamma$ loop. Both $H \to \gamma\gamma$ decay and $\gamma\gamma \to H$ production can be parameterized with the CP-even $a_2^{H\gamma\gamma}$ and CP-odd $a_3^{H\gamma\gamma}$ contributions in Eq. (5) with the ratio $\sigma_2^{H\gamma\gamma}/\sigma_3^{H\gamma\gamma} = 1$ in Eq. (6). However, without access to the photon polarization, it is not possible to distinguish between the two contributions in the $H \to \gamma\gamma$ decay.[1] Therefore, variation of the photon polarization in the photon collider becomes a unique approach to study the CP structure of the $H\gamma\gamma$ vertex.

Three parameters $\mathcal{A}_1, \mathcal{A}_2, \mathcal{A}_3$ sensitive to CP violation have been defined in the context of the photon collider [82–84]. The $\mathcal{A}_1$ parameter can be measured as an asymmetry in the H boson production cross-section between the A_{++} and A_{--} circular polarizations of the beams. This asymmetry is the easiest to measure, but it is proportional to $\Im m(a_2^{H\gamma\gamma} a_3^{H\gamma\gamma\,*})$ and is zero when $a_2^{H\gamma\gamma}$ and $a_3^{H\gamma\gamma}$ are real, as expected for the two loop-induced couplings with heavier particles in the loops. A more interesting parameter,

$$\mathcal{A}_3 = \frac{|A_\parallel|^2 - |A_\perp|^2}{|A_\parallel|^2 + |A_\perp|^2} = \frac{2\Re e(A^*_{--}A_{++})}{|A_{++}|^2 + |A_{--}|^2} = \frac{|a_2^{H\gamma\gamma}|^2 - |a_3^{H\gamma\gamma}|^2}{|a_2^{H\gamma\gamma}|^2 + |a_3^{H\gamma\gamma}|^2} = (1 - 2f_{CP}^{H\gamma\gamma}), \tag{7}$$

can be measured as an asymmetry between two configurations with the linear polarization of the photon beams, one with parallel and the other with orthogonal polarizations.

In Ref. [85], a careful simulation of the process has been performed. The degree of linear polarization at the maximum energies is 60% for an electron beam of energy $E_0 \approx 110\,\text{GeV}$ and a laser wavelength $\lambda \approx 1\,\mu m$. The expected uncertainty on $\mathcal{A}_3$ is 0.11 for $2.5 \cdot 10^{34} \times 10^7 = 250\,\text{fb}^{-1}$ integrated luminosity and $m_H = 120\,\text{GeV}$. This translates to a $f_{CP}^{H\gamma\gamma}$ uncertainty of 0.06, which we enter as an estimate in Table I.

[1] An attempt to measure photon polarization in its conversion is possible [81], but it suffers from a significant loss of statistical precision. We will discuss the photon polarization measurements in the $H \to \gamma^*\gamma^* \to 4f$ process in Section V.

The CP mixture study at a photon collider was also shown based on a sample of 50,000 raw $\gamma\gamma \to H$ events assuming 80% circular polarization of both electron beams [86]. This study corresponds to a $\mathcal{A}_1$ asymmetry measurement, with expected precision on $\mathcal{A}_1$ of about 1%. However, this asymmetry is expected to be zero with real coupling constants $a_2^{H\gamma\gamma}$ and $a_3^{H\gamma\gamma}$ and is therefore of limited interest compared to $f_{CP}^{H\gamma\gamma}$.

IV. PROSPECTS OF HIGGS CP MEASUREMENTS AT A MUON COLLIDER

Similarly to the photon collider, we focus on a unique feature of the muon collider operating at the H boson pole. This allows one to measure the CP structure of the $H\mu\mu$ vertex with the beam polarization in the $\mu^+\mu^- \to H$ process. It is not possible to study the CP structure in the $H \to \mu^+\mu^-$ decay because the muon polarization is not accessible. The muon collider may become the only facility allowing a measurement of CP structure in the H boson's connection to the second-family fermions. At a muon collider operating both at the H boson pole and at higher energy, analysis of the H boson decays is also possible. However, this analysis is similar to the studies performed at other facilities and depends critically on the number of the H bosons produced and their purity.

A. Muon collider at the H boson pole

At a muon collider operating at the resonance pole, the CP quantum numbers of the states can be determined if the muon beams can be transversely polarized. The cross section for production of a resonance takes the form [87]

$$\sigma_{\rm pol}(\zeta) = \sigma_{\rm unpol}\left(1 + P_L^+P_L^- + P_T^+P_T^-\left[\frac{(b_1^{H\mu\mu})^2 - (b_2^{H\mu\mu})^2}{(b_1^{H\mu\mu})^2 + (b_2^{H\mu\mu})^2}\cos\zeta - \frac{2b_1^{H\mu\mu}b_2^{H\mu\mu}}{(b_1^{H\mu\mu})^2 + (b_2^{H\mu\mu})^2}\sin\zeta\right]\right), \tag{8}$$

which depends on P_T (P_L), the degree of transverse (longitudinal) polarization of each of the beams and ζ is the angle of the μ^+ transverse polarization relative to that of the μ^- measured using the direction of the μ^- momentum as the z axis. In particular, muon beams polarized in the same transverse direction selects out the CP-even state, while muon beams polarized in opposite transverse directions (i.e., with spins $+1/2$ and $-1/2$ along one transverse direction) selects out the CP-odd state. A quantitative estimate of the muon collider precision in the measurement of CP structure of the $H\mu\mu$ vertex is left for future studies, which we indicate with a checkmark in Table I.

B. High-energy muon collider

Operation of the muon collider at higher energies will allow access to associated production of the H boson and study CP properties in those processes. Such studies would be similar to those discussed in Sections V and VI and would depend on achieved performance of the muon collider. At energies around 1 TeV, VBF production of the H boson dominates, similarly to the e^+e^- collider. The dominant channel $\mu^+\mu^- \to \nu_\mu\bar{\nu}_\mu(W^+W^-) \to \nu_\mu\bar{\nu}_\mu H$ does not provide kinematic information to analyze the final state with missing neutrinos, but provides H bosons for analysis of their decay. The momentum of the H boson in this VBF production provides sensitivity to the higher-dimension operators, but does not allow one to separate CP-odd and CP-even contributions. The other channel $\mu^+\mu^- \to \mu^+\mu^-(ZZ/Z\gamma^*/\gamma^*\gamma^*) \to \mu^+\mu^- H$ provides sufficient information to analyze potential CP structure in the $HZZ/HZ\gamma/H\gamma\gamma$ couplings. The $t\bar{t}H$ production allows access to CP in the $Ht\bar{t}$ coupling, which is accessible at energies above 0.5 TeV. It is pointed out in Ref. [73] that at energies around 10 TeV, VBF production of $t\bar{t}H$ and $t\bar{q}H$ becomes important. According to Ref. [73], it is expected to achieve constraints on $f_{CP}^{Ht\bar{t}} < 0.67, 0.024$, and 0.003 in three scenarios of the muon collider at 1 TeV with 0.1 ab^{-1} of data, 10 TeV with 10 ab^{-1}, and 30 TeV with 10 ab^{-1}. We do not enter numerical values in Table I due to uncertain muon collider scenarios, but point to the possible measurements with the checkmarks.

V. PROSPECTS OF HIGGS CP MEASUREMENTS AT A HADRON COLLIDER

Hadron colliders provide essentially the full spectrum of possible measurements sensitive to CP violation in the H boson interactions, as outlined in Table I, with the exception of the $H\mu\mu$ vertex. Here we discuss applications to the LHC experiment and its high-luminosity upgrade (HL-LHC), with a proton-proton collision energy around 14 TeV. There is a proposal for a 100 TeV proton-proton collider (FCC-hh or SPPC) which is designed to collect a total luminosity of $20\,\text{ab}^{-1}$. Given increase in the H boson production cross sections by more than an order of magnitude in most production channels, we would expect about two orders of magnitude more H bosons produced and the corresponding increase in precision on f_{CP}^{HX} by between one and two orders of magnitude, given that these measurements are statistics limited, when compared to HL-LHC. Therefore, we expect the 100 TeV pp collider to surpass all other experiments, but we leave only checkmarks in such cases in Table I because detailed simulation studies have not been performed yet and the proposed timescale of this experiment is longer than in most other cases.

A. Gluon fusion process at a hadron collider

The LHC could be considered a gluon collider, as the dominant H boson production mechanism is the gluon fusion $\text{gg} \to H$ process. Many aspects discussed in Section III in application to the photon couplings apply here as well. The coupling of the H boson to two massless gluons is generated by the loops of any massive particles with color charge, which are quarks in the SM. In BSM, new heavy states, either fermions or bosons, could contribute to the loop and generate CP violation. While there is a sizable decay rate $H \to \text{gg}$, study of the gluon polarization is difficult, and within the hadron collider environment this decay mode is hard to distinguish from the dominant QCD background. However, study of the gluon fusion process in the scattering topology of the H boson production in association with two hadronic jets allows access to the CP property of the $H\text{gg}$ vertex [39]. This VBF topology is illustrated in the first diagram of Fig. 1, where $V^* = \text{g}$.

Similarly to the photon couplings, the gluon fusion process can be characterized by the two couplings CP-even $a_2^{H\text{gg}}$ and CP-odd $a_3^{H\text{gg}}$, which absorb both SM and heavy BSM particles in the loop. While in the EFT approach, these contributions could be disentangled in a global fit of multiple processes, this is not possible with the gluon fusion process alone. Therefore, we parameterize the CP violation effects with a single parameter $f_{CP}^{H\text{gg}}$. In order to isolate CP-sensitive effects, no constraint on the process rate is applied, which is proportional to $|a_2^{H\text{gg}}|^2 + |a_3^{H\text{gg}}|^2$.

The Snowmass-2013 projection [76] was based on the study of the $\text{gg} \to H$ process with $H \to 4\ell$ [52]. Since then, this approach was successfully applied on LHC [20, 22, 24] using $140\,\text{fb}^{-1}$ of data, with the results in good agreement with the above expectation. For example, the constraint $f_{CP}^{H\text{gg}} < 0.26$ at 68% C.L. is expected with $H \to \tau\tau$ and 4ℓ combined [24], which would scale to $f_{CP}^{H\text{gg}} < 0.011$ with $3000\,\text{fb}^{-1}$, as shown in supplemental materials [88], and $f_{CP}^{H\text{gg}} < 0.12$ with $300\,\text{fb}^{-1}$, where the improvement with respect to the Snowmass-2013 projection is due to an additional H boson decay channel analyzed. Somewhat more conservative results are projected in Ref. [69]. Therefore, in Table I, we estimate that $f_{CP}^{H\text{gg}} < 0.011$ could be achieved with $3{,}000\,\text{fb}^{-1}$, but note that further improvement is very likely, both from the inclusion of multiple decay channels and from improvements in experimental analyses.

B. The $H\gamma\gamma$ and $HZ\gamma$ couplings at a hadron collider

While the $H \to \gamma\gamma$ decay was one of the two primary H boson discovery channels, this decay process does not allow access to CP structure of the photon couplings, as discussed in Section III. Similarly, the $H \to Z\gamma$ decay does not provide access to CP structure of the $HZ\gamma$ vertex when the couplings in Eq. (5) are real. Complex couplings could be generated with light particles in the loop, for example, and could generate forward-backward asymmetry in the polar angle, as shown in Ref. [52], but we do not consider such a possibility here. Another approach, suggested in Ref. [89], relies on complex phases generated through different Breit-Wigner propagators in the interference of the γ^* and Z contributions in the decay $H \to \ell^+\ell^-\gamma$ process. However, this approach is not necessarily better than $H \to 4\ell$, which includes $H \to \ell^+\ell^-(\gamma^*/Z)$, and would require further feasibility studies.

However, several other topologies may allow access to the CP structure of the $H\gamma\gamma$ and $HZ\gamma$ couplings. These include

1. the VBF process: $qq' \to qq'(\gamma^*\gamma^*/Z\gamma^*) \to qq'H$,
2. the VH process: (a) $q\bar{q} \to \gamma^*/Z \to \gamma^*H/ZH \to (2f)H$, (b) $q\bar{q} \to \gamma^*/Z \to \gamma H$,
3. the 4/3/2-body decays: (a) $H \to \gamma^*\gamma^*/Z\gamma^* \to 4f$, (b) $H \to \gamma\gamma^*/\gamma Z \to \gamma(2f)$, (c) $H \to \gamma\gamma$.

It is important to note that the above processes do not appear in isolation and whenever γ^* appears in the intermediate state, Z^* appears as well, leading to interference. For example, the full analysis of the process $H \to \gamma^*\gamma^*/\gamma^*Z/ZZ \to 4f$ may allow access to CP violation through interference of the CP-odd $a_3^{HZ\gamma}$ term with the dominant CP-even a_1^{HZZ} term appearing at tree level, and this needs to be disentangled from the possible $a_3^{H\gamma\gamma}$ and a_3^{HZZ} terms. Therefore, the full analysis of each process requires accounting for all contributions, including the HZZ couplings discussed in Section V C.

The three LHC topologies which involve the $H\gamma\gamma$ and $HZ\gamma$ couplings are shown in Fig. 1, where $V^* = \gamma^*$ or Z. The processes with onshell photons can also be represented by the diagrams (2) and (3) in Fig. 1 with $V^* = \gamma$, but with no subsequent decay of the photon. However, these processes with onshell photons do not allow access to CP effects without the measurement of the onshell photon polarization, unless complex anomalous couplings are considered. Illustration of CP-sensitive effects with complex couplings appearing in the forward-backward asymmetry of the angular distributions can be found for $q\bar{q} \to Z^* \to \gamma H$ in Ref. [71] and $H \to \gamma Z \to \gamma(2f)$ in Ref. [52]. An angle Φ identified in all three diagrams in Fig. 1 is an angle between the decay or production planes defined by the four four-momenta and is the primary CP-odd observable in each process. However, a multivariate analysis of the full kinematic information leads to the most optimal amplitude analysis, which is sensitive to both squared and interference of the CP-odd and CP-even terms.

An attempt to study the CP structure of the $H\gamma\gamma$ and $HZ\gamma$ couplings in the golden channel $H \to 4\ell$ was performed at the LHC in Ref. [7], where it became clear that reaching an interesting level of sensitivity will require very high luminosity. The $H\gamma\gamma$ couplings in the $H \to 4\ell$ decay were considered phenomenologically in Ref. [59]. More recently, a joint analysis of the three processes VBF, VH, and decay $H \to 4\ell$ was investigated in Ref. [71], where it was shown that while the decays $H \to \gamma\gamma$ and $H \to Z\gamma$ are most sensitive to the overall strength $|a_2^{H\gamma\gamma}|^2 + |a_3^{H\gamma\gamma}|^2$ and $|a_2^{HZ\gamma}|^2 + |a_3^{HZ\gamma}|^2$, the decay $H \to 4\ell$ process is most sensitive to study the tensor structure of the $H\gamma\gamma$ and $HZ\gamma$ couplings, relevant for CP violation measurements. We should note that in all the above studies, the effective values of $a_2^{H\gamma\gamma}$ and $a_2^{HZ\gamma}$ which reproduce the SM rate of $H \to \gamma\gamma$ and $H \to Z\gamma$ decays were used to approximate the SM processes $H \to \gamma^*\gamma^*/Z\gamma^* \to 4\ell$, VBF, and VH. While this prescription is not technically correct to represent the SM rate due to q^2 dependence of the couplings, this simulated value of a_2 is a good benchmark for the Snowmass exercise as it is used only as a reference to estimate sensitivity to a_3. The results of the study in Ref. [71] are reinterpreted in terms of $f_{CP}^{H\gamma\gamma}$ and $f_{CP}^{HZ\gamma}$ in Appendix A and are entered in Table I. The full dataset of the HL-LHC will be at the boundary to start setting meaningful constraints on these parameters.

Given the difficulty to set CP constraints on the $H\gamma\gamma$ and $HZ\gamma$ couplings at HL-LHC, exploring other options might be useful. A possible study of $H \to \gamma\gamma \to 4e$ with photon polarization in its conversion has been suggested in Ref. [81], but this study suffers from a significant loss of statistical precision, and a more detailed study of experimental aspects, such as reconstruction of displaced and boosted e^+e^- pairs with a small opening angle, may be required.

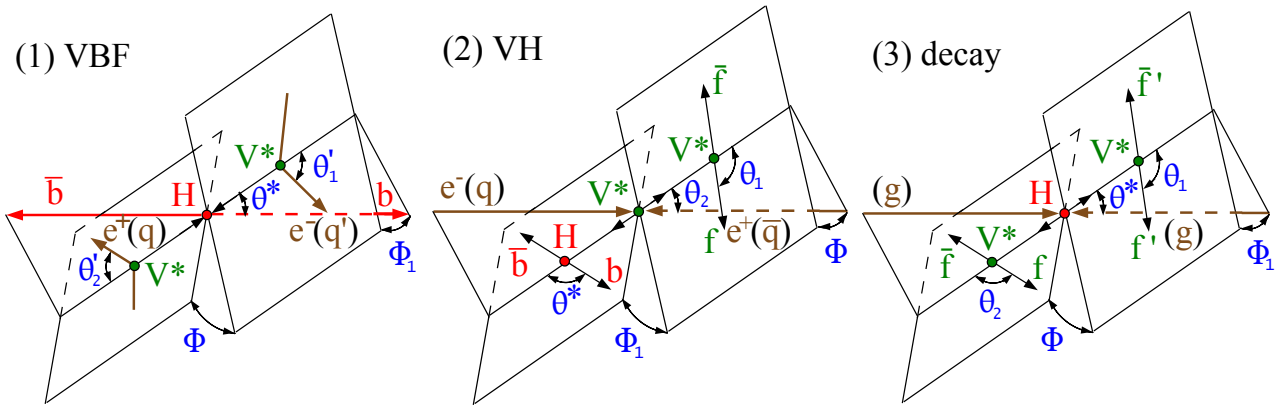


FIG. 1: Illustrations of the H boson kinematic observables in pp, e^+e^-, or $\mu^+\mu^-$ collision in (1) the VBF process: $e^+e^-(qq') \to e^+e^-(qq')H \to e^+e^-(qq')b\bar{b}$; (2) the VH process: $e^+e^-(q\bar{q}) \to V^* \to V^*H \to f\bar{f}b\bar{b}$; and (3) the decay: $gg \to H \to V^*V^* \to 4f$. Five angles fully characterize the orientation of the production and decay chain and are defined in the suitable rest frames. The diagrams are adopted from Refs. [43, 52].

C. The HZZ and HWW couplings at a hadron collider

The HZZ and HWW couplings appear at tree level in the SM and the decays $H \to ZZ \to 4f$ and $H \to W^+W^- \to 4f$ provided rich kinematic information for studies of spin and CP properties of the H boson in the early days after the H boson discovery and have historically been studied extensively on LHC experiments [4–13, 15, 16, 19, 20, 22–24]. However, with the growing significance of the H boson electro-weak production (VBF and VH), the larger q^2 values tested lead to stronger constraints of CP effects in these production modes. The three main topologies involving the HZZ and HWW couplings follow closely those in Section V B and appear in Fig. 1, with $V^* = Z$ or W, as

1. the VBF process: $qq' \to qq'(W^+W^-/ZZ) \to qq'H$,
2. the VH process: (a) $q\bar{q} \to Z \to ZH \to (2f)H$, (b) $q\bar{q}' \to W^\pm \to W^\pm H \to (2f)H$,
3. the 4-body decay: (a) $H \to ZZ \to 4f$, (b) $H \to W^+W^- \to 4f$.

All processes with the Z boson interfere with the same processes involving γ^* in its place, as listed in Section V B. We note that the process gg $\to VH$ also receives attention due to the large gluon luminosity in proton collisions. This channel provides an interesting interplay of $Hf\bar{f}$ and HVV couplings, but does not have contribution from the CP-odd terms with $a_3^{HZZ}, a_3^{HZ\gamma}$, or $a_3^{H\gamma\gamma}$ [69], and therefore is not suitable for studies of CP violation in $HZZ, HZ\gamma$, or $H\gamma\gamma$ interactions.

Even though the HZZ and HWW couplings can be easily analyzed separately in the ZH vs. WH production with leptonic Z or W decay, or in $H \to ZZ$ vs. $H \to WW$ decays, it is essentially impossible to disentangle those in the VBF production, where all kinematic features are nearly identical. The tree-level couplings HZZ and HWW can be related through custodial symmetry, leading to $a_1^{HZZ} = a_1^{HWW}$. Within the precision of the H boson measurements, this relationship is not significantly affected by the recent tension in the W mass measurements. The anomalous HZZ and HWW couplings, such as a_3^{HZZ} and a_3^{HWW}, could also be related through symmetry, such as $SU(2) \times U(1)$. For example, $a_3^{HWW} = a_3^{HZZ} \cdot \cos^2\theta_W$ if contributions of the $H\gamma\gamma$ and $HZ\gamma$ couplings are neglected. Most of the experimental studies on LHC and projections of the feasibility studies have been performed under such or a similar relationship of the HZZ and HWW couplings. Therefore, in Table I we estimate precision on f_{CP}^{HVV} which represents $V = Z$ and W combined.[2] Precision of the separate measurements would be less, but similar. We should also note that since a_1^{HZZ} and a_1^{HWW} are generated at tree level in the SM, they are expected to be much larger than a_3^{HZZ} and a_3^{HWW}, which appear at loop level, similar to the photon couplings. Therefore, the interesting values of f_{CP}^{HVV} are much smaller than those for f_{CP}^{Hgg}, $f_{CP}^{H\gamma\gamma}$, and $f_{CP}^{HZ\gamma}$, as reflected in the last column of Table I.

The Snowmass-2013 projections [76] were split into the study of the HVV couplings in three processes: $H \to 4\ell$ decay, VBF production with $H \to \gamma\gamma$, and VH production with $H \to b\bar{b}$ [52], where the most powerful channels were picked in each case. In the present study, we do not separate the channels and consider the combined or best performance, assuming that the effective field-theoretic description does not breakdown with the q^2 growth. Several experimental updates with $140\,\text{fb}^{-1}$ of LHC data have appeared since then, some of the recent ones include Refs. [20, 24], where the constraint $f_{CP}^{HVV} < 8 \times 10^{-5}$ is expected at 68% C.L. from analysis of electroweak production information in the $H \to \tau\tau$ and 4ℓ channels. The H boson physics projections at the HL-LHC and HE-LHC were revised in Ref. [90], where Fig. 38 indicates $f_{CP}^{HVV} < 0.037$ from $H \to 4\ell$ and Fig. 39 indicates $f_{CP}^{HVV} < 1.8 \times 10^{-4}$ at 95% C.L. from production with $H \to 4\ell$ at $3{,}000\,\text{fb}^{-1}$ When a combined analysis of the $H \to \tau\tau$ and 4ℓ channels is used, the expectation is $f_{CP}^{HVV} < 2.5 \times 10^{-6}$ at 68% C.L. at $3{,}000\,\text{fb}^{-1}$, as shown in supplemental materials [88]. We use these studies to indicate that $f_{CP}^{HVV} < 2.5 \times 10^{-6}$ at $3{,}000\,\text{fb}^{-1}$ and $f_{CP}^{HVV} < 4.0 \times 10^{-5}$ at $300\,\text{fb}^{-1}$ are achievable at 68% C.L. Further improvements are likely from the inclusion of multiple decay channels and from improvements in experimental analyses.

D. The $Ht\bar{t}$ coupling at a hadron collider

The CP structure of the H boson couplings to fermions is particularly interesting because both CP-even and CP-odd components can appear at tree level, and therefore the $f_{CP}^{Hf\bar{f}}$ values do not necessarily need to be very small. (This is in contrast to f_{CP}^{HVV}, for example.) One could get access to the $Hf\bar{f}$ interactions through loops appearing in the Hgg, $H\gamma\gamma$, and $HZ\gamma$, but we treat those separately in Sections V A and V B because one cannot disentangle loop

[2] Technically, f_{CP}^{HVV} is defined for $H \to ZZ \to 2e2\mu$ with $\sigma_1^{HZZ}/\sigma_3^{HZZ} = 6.54$ in Eq. (6), but the measurement relies on both HZZ and HWW couplings.

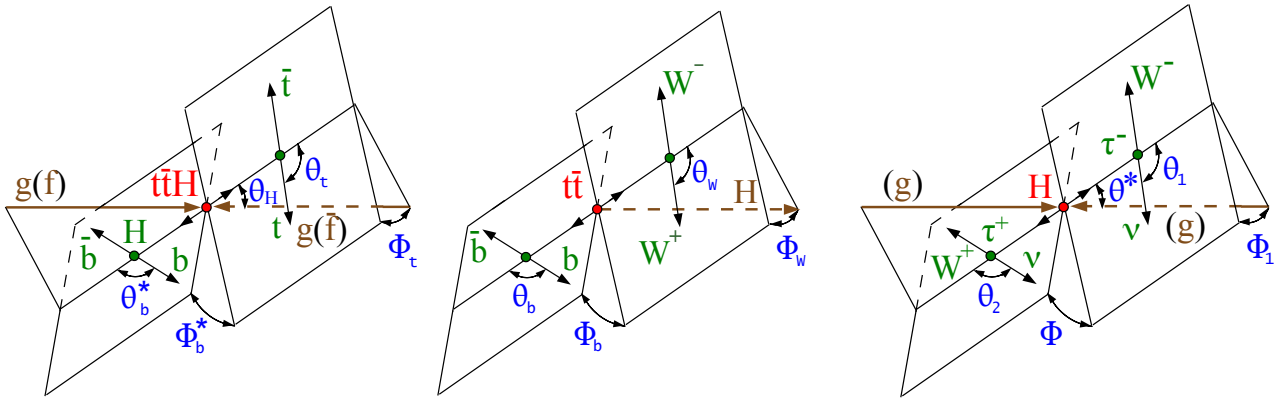


FIG. 2: Illustrations of the H boson kinematic observables in pp, e^+e^-, or $\mu^+\mu^-$ collisions in (left and middle) the $t\bar{t}H$ process with sequential decay; (right) the $H \to \tau^+\tau^-$ decay process. The subsequent W decay is not shown. The b and W pairing in the $t\bar{t}$ decays is switched to enhance visibility of CP effects in individual angular observables. The diagrams are adopted from Ref. [62].

contributions without a global analysis. A measurement of the CP structure of the H boson couplings to the first- and second-family fermions is essentially impossible at a hadron collider, as there are no channels where polarization measurements could be performed. A CP measurement of the $Hb\bar{b}$ vertex is also essentially impossible, as neither $H \to b\bar{b}$ decay nor $b\bar{b}H$ production allows access to CP [62] without the polarization measurements of the b quarks, which, if attempted in their decays, suffer from significant loss of statistical precision. This leaves only the $Ht\bar{t}$ and $H\tau\tau$ couplings with CP structure that can be measured at a hadron collider.

The $t\bar{t}H$ production process has received the primary attention on LHC as the channel to study CP the structure of the $Ht\bar{t}$ coupling [34, 58, 60, 62, 70, 72, 73], while the tqH and tWH processes also allow access to CP in this coupling. The cross sections of the latter channels are smaller, but they feature interference of the $Ht\bar{t}$ and HVV couplings, which help in resolving the sign ambiguity in the relative phase, and a joint analysis of all these channels is often required due to cross-feed of events in analysis of the data. There is also a proposal to access CP-violating effects in $Ht\bar{t}$ couplings through loop effects in $t\bar{t}$ production [70], but the precision of such constraints does not alter our conclusion drawn from channels with associated H boson production. There is rich kinematic information in the sequential decay of the particles produced in association with the H boson in the $t\bar{t}H$, tqH, and tWH processes, as indicated in the two diagrams in Fig. 2. However, most information is sensitive to the square of the CP-odd and CP-even amplitudes.

It is also possible to construct CP-odd observables that are sensitive to the interference term in the amplitude by exploring the $t\bar{t}$ spin correlations. These spin correlations can be traced back from the decay products of t and $\bar{t}$, since the top-quark lifetime ($\sim 10^{-25}$ s [91]) is much shorter than the time required for spin decorrelation effects to actualize ($\sim 10^{-21}$ s) [92]. Thus, CP-odd observables can be constructed from antisymmetric tensor products of the four-momenta of the top, anti-top, and their respective decay products i and k, $\epsilon(p_t, p_{\bar{t}}, p_i, p_k) \equiv \epsilon_{\mu\nu\rho\sigma} p_t^\mu p_{\bar{t}}^\nu p_i^\rho p_k^\sigma$. In the $t\bar{t}$ rest frame, this antisymmetric tensor product can be simplified to $\vec{p}_t \cdot (\vec{p}_i \times \vec{p}_k)$, which can be used to define genuine CP-sensitive azimuthal angle differences [93, 94]. Correlations between two decay products, one from t and the other from $\bar{t}$, scale with the spin analyzing power (β_i) associated with the decay product [95]. Charged leptons and down-type quarks exhibit the highest spin correlations $|\beta_i| = 1$, followed by bottom quarks and W bosons with $|\beta_i| = 0.4$, and neutrinos and up-type quarks with $|\beta_i| = 0.3$. Therefore, one would require access to the flavors of the fermions and anti-fermions in the subsequent t/W^+ and $\bar{t}/W^-$decays to probe the interference. This is possible in the leptonic decays of both W's in the $t\bar{t}$ decay, but statistical precision in this fully leptonic channel is significantly weaker than in the semi-leptonic and fully-hadronic channels.

Both the CMS and ATLAS experiments [17, 18, 20, 25, 26] have performed an amplitude analysis of the CP-even and CP-odd components of the $Ht\bar{t}$ coupling analyzing both $t\bar{t}H$ and tH processes. One of the dominant H boson decay channels is $H \to \gamma\gamma$, but other decays can also make significant contributions. Only semi-leptonic and fully-hadronic top decays in the $t\bar{t}H$ channels have been used, therefore limiting CP analysis to the square of the amplitudes. With about 140 fb^{-1} of LHC data, a single experiment obtained an expected sensitivity of $f_{CP}^{Ht\bar{t}} < 0.5$ at 68% C.L. with $H \to \gamma\gamma$ [17] and of $f_{CP}^{Ht\bar{t}} < 0.35$ in combination with the multi-lepton H boson decays [25]. Phenomenological studies indicate $f_{CP}^{Ht\bar{t}} < 0.4$ at 300 fb^{-1} in Ref. [62] using the $H \to \gamma\gamma$ channel. Exploring the same H boson final state together with combined searches in the semi-leptonic, di-leptonic, and fully-hadronic top quark pair decays, the study in Ref. [72] indicates a sensitivity of $f_{CP}^{Ht\bar{t}} < 0.05$ at the HL-LHC with 3,000 fb^{-1}. Despite larger rates, searches in

the $pp \to t\bar{t}(H \to b\bar{b})$ channel leads to typically weaker projections due to an imposing QCD background, which is also marred by substantial systematic uncertainties [93, 94]. The diphoton channel stands at a vantage point due to controlled backgrounds facilitated by data-driven side-bands. Inclusive and differential H boson measurements were investigated in Ref. [96] and full kinematic information was investigated phenomenologically in Ref. [97], leading to similar expectations. We enter $f_{CP}^{Ht\bar{t}} < 0.24$ at $300\,\text{fb}^{-1}$ and < 0.05 at $3{,}000\,\text{fb}^{-1}$ in Table I and note that further improvements are expected from analysis of other H boson decay channels.

E. The $H \to \tau^+\tau^-$ process at a hadron collider

The $H \to \tau^+\tau^-$ decay is an excellent probe of spin correlation in the sequential decay of the two taus. For example, an angle between the two decay planes indicated in Fig. 2 is sensitive to CP in the $H\tau\tau$ interaction. However, this angle cannot be measured directly due to missing neutrinos, and the experimental challenge is to approximate it with available information. For example, the pion is preferably emitted in the direction of the τ spin in the τ rest frame, and additional information, such as the tau decay impact parameter, help to reconstruct CP-sensitive observables.

At the time of the Snowmass-2013 studies [76], it was believed that this reconstruction would be challenging, though possible, in the hadron collider environment [98]. Most studies were focussed on the cleaner e^+e^- collider environment, discussed in Section VI D. A study in Ref. [99] using an optimal observable based on the internal substructure of $\tau^\pm \to \pi^\pm\pi^0\nu$ indicated sensitivity to $f_{CP}^{H\tau\tau} < 0.04$ at $3{,}000\,\text{fb}^{-1}$ integrated luminosity of HL-LHC. However, it was found in Ref. [100] that detector effects would be more important than originally suggested. A realistic study by the ATLAS collaboration [101] was based on analysis of $\tau^\pm \to \pi^\pm\pi^0\nu$ and indicated that at HL-LHC the statistical precision on $f_{CP}^{H\tau\tau}$ would range between 0.10 and 0.30, depending on the precision of the π^0 reconstruction. Finally, a very detailed study of multiple τ decay channels by the CMS experiment [21] achieved an expected precision of $f_{CP}^{H\tau\tau} < 0.13$ at 68% C.L. with about $140\,\text{fb}^{-1}$. A similar recent study by ATLAS [27] leads to $f_{CP}^{H\tau\tau} < 0.22$ at 68% C.L. The CMS experiment provided projection to $3{,}000\,\text{fb}^{-1}$ as supplemental materials [102] to Ref. [21], from which we expect $f_{CP}^{H\tau\tau} < 0.07$ at $300\,\text{fb}^{-1}$ and < 0.008 at $3{,}000\,\text{fb}^{-1}$, which are entered in Table I.

VI. PROSPECTS OF HIGGS CP MEASUREMENTS AT AN ELECTRON-POSITRON COLLIDER

Many of the approaches to the H boson CP measurements at an electron-positron collider are similar to those at a hadron collider, but with several notable features. First, the e^+e^- collider environment is much cleaner, and therefore even with a smaller number of H bosons produced, essentially every final state of its decay may be used for tagging. Second, certain final states, most notably $\tau^+\tau^-$, could be reconstructed and analyzed for CP structure with better efficiency. Third, the fixed initial-state energy in the $e^+e^- \to V^* \to VH$ production allows control over the q^2 of the initial V^*. Similarly, possible polarization of the colliding beams may give additional control in polarization measurements.

The CP structure of the H boson couplings to gluons cannot be easily measured at a lepton collider, because the decay to two gluons does not allow easy access to gluon polarization. On the other hand, most other processes could be studied at an e^+e^- collider, especially with the beam energy above the $t\bar{t}H$ threshold.

A. The VH process at an electron-positron collider

The $e^+e^- \to ZH/\gamma^*H \to (2f)H$ process is the dominant SM process at lower energies with cross section of about 240/129/57/13 fb at $\sqrt{s} = 250/350/500/1{,}000\,\text{GeV}$. Full angular analysis of the final state allows access to CP information. Similarly to the hadron collider, the process $e^+e^- \to \gamma H$ is possible to study, but does not allow access to CP properties from the angular analysis. This channel has been used at LEP to set constraints on the H boson production with possible anomalous $HZ\gamma$ and $H\gamma\gamma$ couplings.

An early feasibility study of spin-parity determination and analysis of the HZZ and $HZ\gamma$ coupling tensor structure in the VH process at an e^+e^- collider was performed as part of the TESLA design [103] based on 300 fb^{-1} at a centre-of-mass energy of 500 GeV and $m_H = 120$ GeV. The Snowmass-2013 studies [76] relied on Ref. [52], which compared the expected performance of an e^+e^- collider and the LHC, with the $H \to b\bar{b}$ and $Z \to \ell\ell$ decays used in the former case. Precision on the fraction of the CP-odd cross-section contribution of about 0.03 was obtained across the four energy and luminosity scenarios. The significant reduction in the f_{CP}^{HVV} uncertainties with energy is due to the increase of the q^2 of intermediate Z, and therefore higher relative contribution of the higher-dimension operators to the production cross section, where it is assumed that no strong momentum dependence of couplings occurs at these energies. A recent update of these studies in Appendix B produced expected constraints with the

same luminosity scenarios and with an order of magnitude higher integrated luminosity, which are consistent within a factor of two with the more recent recommendations for Snowmass-2022 studies, as outlined in Ref. [80]. A study of beam polarization effects is also included in Appendix B.

There were no separate studies of the precision on $f_{CP}^{HZ\gamma}$ or $f_{CP}^{H\gamma\gamma}$ at the time of the Snowmass-2013 studies [76], but a recent update of these studies in Appendix B indicate that it is not feasible to constrain $f_{CP}^{HZ\gamma}$ or $f_{CP}^{H\gamma\gamma}$ at an e^+e^- collider with parameters listed in Table I. Only the $f_{CP}^{Z\gamma}$ parameter at E = 1 TeV and $\mathcal{L} = 10\,\text{ab}^{-1}$ allows a non-trivial constraint at 68% C.L., as indicated in the last column of Table III in Appendix B, but still with essentially 100% uncertainties. Of course, should there be an anomalously large $H\gamma\gamma$ or $HZ\gamma$ coupling, much larger than expected from loop effects in the SM, one could isolate CP-odd contributions with a relatively high precision, but such a scenario is excluded by the rates of the $H \to \gamma\gamma$ and $H \to Z\gamma$ processes.

The CP-odd HZZ and $HZ\gamma$ couplings have been investigated with $5.6\,\text{ab}^{-1}$ at 240 GeV with $Z \to \mu^+\mu^-$ and $H \to b\bar{b}, c\bar{c}$, gg in Ref. [104], which follows closely similar earlier studies in Refs. [105, 106]. The expected constraint on the CP-odd $HZ\gamma$ coupling $a_3^{Z\gamma}$ is about a factor of six larger than the SM $a_2^{Z\gamma}$ expectation [71], which indicates that it is hard to constrain photon couplings in this process, in agreement with the conclusion reached above about $f_{CP}^{HZ\gamma}$ or $f_{CP}^{H\gamma\gamma}$.

The expected constraint on the CP-odd HZZ coupling a_3^{ZZ}, which is equivalent to $\tilde{c}_{zz}$ used in Ref. [104], can be translated to the expectation $f_{CP}^{HVV} < 3.7{\cdot}10^{-4}$ at 68% C.L. assuming that this limit scales linearly with luminosity (or square root of luminosity for the coupling). This appears to be similar to the Snowmass-2013 expectation and in agreement with the constraint obtained in Appendix B, $f_{CP}^{HVV} < 3.4 \cdot 10^{-4}$. The expected constraints obtained at three other energy and luminosity scenarios in Appendix B are nearly identical to those obtained in the Snowmass-2013 studies [52, 76] and we keep those unchanged. We also consider an order of magnitude higher luminosity in Appendix B.

It has been pointed out in Ref. [107] that in addition to the process $e^+e^- \to ZH$ with $Z \to \ell\ell$ (7%), one can use the $Z \to q\bar{q}$ (70%) final states. While both reconstruction and backgrounds will be somewhat more challenging with hadronic jets, the larger branching fraction will make the hadronic channel dominate. We have not included results from Ref. [107] in our projections in Table I, because the comparison to other projections is not fully resolved, but we point out that in the most optimistic scenario, the final state $Z \to q\bar{q}$ provides an order of magnitude increase in the available data, and the expected results would correspond to a ten times larger luminosity scenario in Appendix B. Therefore, in the summary Table I, we enter results from Table III corresponding to the $Z \to \ell\ell$ channel, but with a ten times larger luminosity. When it comes to a comparison of HL-LHC and e^+e^- projections, where typically only one H boson decay channel is analyzed at HL-LHC (e.g. $H \to \tau^+\tau^-$), the inclusion of other channels (e.g. $H \to b\bar{b}, \gamma\gamma, W^+W^-, ZZ$) will increase the available data by a factor of 5 or so.

B. The VBF process at an electron-positron collider

VBF production with charged boson fusion $e^+e^- \to \nu_e\bar{\nu}_e(W^+W^-) \to \nu_e\bar{\nu}_e H$ is the dominant SM process at higher energies with cross section of 21/34/72/210 fb at $\sqrt{s} = 250/350/500/1,000$ GeV. However, there is essentially no kinematic information to analyze in the final state with missing neutrinos, with the exception of the momentum of the H boson, which provides sensitivity to the higher-dimension operators, but does not allow one to separate CP-odd and CP-even contributions. Therefore, this channel is useful to study CP in the subsequent H boson decays, though the lack of a vertex from associated particles makes certain techniques less reliable, as discussed in application to $H \to \tau^+\tau^-$ for example.

VBF production with neutral boson fusion $e^+e^- \to e^+e^-(ZZ/Z\gamma^*/\gamma^*\gamma^*) \to e^+e^-H$ cross section is smaller than of the main VBF channel with associated neutrinos, but is still sizable at higher energies with the SM cross section of $0.7/3/7/21$ fb at $\sqrt{s} = 250/350/500/1,000$ GeV. Full angular analysis allows access to CP information. For example, an ongoing study of the ZZ-fusion process at 1.4 TeV CLIC and 1 TeV ILC are mentioned in Ref. [108], and the first preliminary estimates have been shown at ICHEP-2022 conference [109]. However, the precision in this channel at these intermediate energies does not surpass that expected from the $e^+e^- \to ZH \to (2f)H$ process, and therefore Table I is not affected. While there is no dedicated study of the CP-odd $H\gamma\gamma$ and $HZ\gamma$ interactions in VBF production $e^+e^- \to e^+e^-(ZZ/Z\gamma^*/\gamma^*\gamma^*) \to e^+e^-H$, an analogy has been drawn to the VBF process at LHC in Appendix B, which indicates that it is unlikely that $f_{CP}^{HZ\gamma}$ or $f_{CP}^{H\gamma\gamma}$ could be constrained at an e^+e^- collider.

C. The $t\bar{t}H$ process at an electron-positron collider

H boson production in association with top quarks $e^+e^- \to t\bar{t}H$ is the fourth production channel for energies above the threshold around 500 GeV, with cross section of 0.27/2.0 fb at $\sqrt{s} = 500/1,000$ GeV. Many of the techniques used at the LHC in Section V D and at a muon collider in Section IV B can be employed at an e^+e^- collider, with the diagram in Fig. 2 representating kinematic information in the process.

A study of *CP*-odd contribution in the $Ht\bar{t}$ coupling has been studied in the context of ILC [76]. Cross-section dependence on the coupling has been employed and an uncertainty on f_{CP}^{Htt} of 0.08 (0.29) at 1,000 (500) GeV center-of-mass energy has been estimated. A beam polarization of $(+0.2, -0.8)$ [110] and $(+0.3, -0.8)$ is assumed at 1,000 and 500 GeV, respectively. A more recent study indicates sensitivity to f_{CP}^{Htt} of about 0.07 expected with 2,000 fb^{-1} and 1,400 GeV [111], which employs a similar cross section dependence. Interpretation of a cross-section deviation as an indication of *CP*-odd coupling contribution is strongly model-dependent, but allows access to anomalous $Ht\bar{t}$ couplings. An analysis of the full kinematic information could proceed in a manner similar to that employed at LHC and would benefit from the clean e^+e^- collider environment with the beam energy constraints available. An improvement from using the differential information has been observed in Ref. [112].

D. The $H \to \tau^+\tau^-$ and other decay processes at an electron-positron collider

At the time of the Snowmass-2013 exercise [76], most CP studies with $H \to \tau^+\tau^-$ were performed in a clean e^+e^- environment, either in the decays $\tau \to \pi\pi\nu$ [99, 113], or in all final states [114, 115]. All studies agree on a similar $f_{CP}^{H\tau\tau}$ precision of about 0.01 for the typical scenarios in Table I. The precision becomes somewhat worse with an increased collider energy due to the reduced ZH production cross-section, and this technique relies on the knowledge of the Z vertex. A recent full simulation study of the ILC physics reach with 1,000 fb^{-1} at 250 GeV indicates a very similar $f_{CP}^{H\tau\tau}$ precision of about 0.01 with $\tau^\pm \to \pi^\pm\nu$ and $\tau^\pm \to \pi^\pm\pi^0\nu$[108, 116], but additional τ lepton decays may bring an increase in sensitivity. We therefore leave the estimates in Table I the same as in the Snowmass-2013 projection. Further improvements could be achieved using the lessons learned from the realistic analysis of the $H \to \tau^+\tau^-$ channel at LHC, as discussed in Section V E.

Analysis of the other decay channels, most notably $H \to 4f$, could be performed at an e^+e^- collider. The clean collider environment would allow exploration of multiple final states, beyond just the golden channels with charged leptons used at LHC. However, as noted in Appendix B, the number of produced $H \to ZZ \to 4f$ events at an e^+e^- collider would be significantly smaller than the number of H bosons produced in the golden clean channel $H \to 4\ell$ at a proton collider.

The e^+e^- collider may become a clean environment for studies of the other two-body final states involving hadronic decays, though their polarization measurements would be challenging. In Section V D, we have already mentioned that in the $H \to b\bar{b}$ decay, a polarization measurement of the b-quark jets may allow measurement of the CP structure of the $Hb\bar{b}$ vertex. Similarly, in the $H \to$ gg decay, a polarization measurement of the gluon jets may allow a CP measurement in the Hgg coupling. Feasibility studies of both measurements in realistic experimental environment need to be performed.

VII. PROSPECTS OF HIGGS CP MEASUREMENTS AT A LEPTON-HADRON COLLIDER

The electron-proton collider allows production of the H boson in the VBF topology and top-associated production in a relatively clean environment, without the complications arising from pile-up typical of hadron colliders [117]. Three main production mechanisms include VBF production of an H boson and a quark jet in association with a neutrino $\nu_e Hq$ or an electron $e^- Hq$, and single-top-quark associated production $\nu_e H\bar{t}$. For the beam energies of $E_p = 7$ TeV and $E_e = 60$ GeV, corresponding to $\sqrt{s} = 1.3$ TeV, the cross sections of the these processes are 0.197 pb, 0.024 pb, and 0.002 pb [117]. Therefore, with about 1 ab of integrated luminosity, more than 200,000 H bosons can be produced.

A. The VBF process at a lepton-hadron collider

In VBF production, WW and $ZZ/Z\gamma^*/\gamma^*\gamma^*$ fusion can be easily separated with the signature $e^- p \to \nu_e Hq$ (charged current) or $e^- p \to e^- Hq$ (neutral current), respectively. Studies of these processes [118–120] have been performed without consideration of the photon couplings. However, similarly to the VBF process at a proton-proton collider

discussed in Appendix A, we would expect the photon couplings $H\gamma\gamma$ and $HZ\gamma$ to have weak constraints. The most recent projections of constraints on the HWW and HZZ CP-odd couplings have been reported in Ref. [120].

B. The top-H process at a lepton-hadron collider

The top Yukawa coupling has been studied in the $e^-p \to \nu_e H\bar{t}$ process in Ref. [121]. There is an interference between the diagrams with the HWW and Hbb/Htt couplings. The cross section of this process exhibits a dependence on the faction of the CP-odd component in the Htt interaction. This dependence has been explored in Ref. [121]. However, a study which considers variation of more than one parameter and using CP-sensitive observables would be desired. In Table I, we indicate that a study of the Htt and HZZ/HWW interactions is possible at an e^-p collider. It would be also interesting to investigate if there is a sensitivity to CP structure in the Hbb interaction.

VIII. COMPARISON TO EDM MEASUREMENTS

A dedicated Snowmass-2022 study of EDM measurements can be found in Ref. [122]. Asymmetry in the charge distribution along the particle's spin requires T violation, which is equivalent to CP violation when invoking the CPT theorem. The EDMs of atoms and molecules are sensitive to CP violation in interactions of the H boson through loop effects. The SM values of these EDMs are beyond the current or planned experimental reach, which allows excellent null tests in the SM. The EDM constraints on CP-odd H boson couplings are typically stronger than those from direct H boson measurements [123–127]. However, these constraints are set under an assumption that only one modification of the H boson coupling is present in the loop, and therefore no cancellation effect is allowed. With multiple CP-odd EFT operators, the EDM measurements set constraints on certain linear combinations of these operators, and direct constraints on the CP-odd operators in the H boson measurements provide complementary information.

For example, the $H\gamma\gamma$, $HZ\gamma$, HZZ, as Hgg induce EDMs through one-loop diagrams. Replacing the HVV vertex with a fermion loop in these diagrams leads to two-loop graphs, through which the Hff couplings can contribute. One can also analyze these interactions with simultaneous contributions of loops of SM particles together with BSM interactions and point-like HVV interactions generated by heavy BSM states. At the same time, the second vertex of the H boson involves $Hu\bar{u}$, $Hd\bar{d}$, or Hee interactions, where CP violation could be introduced as well. Therefore, in general, EDMs receive contributions from a large number of CP-odd interactions, allowing for the possibility of cancellations. While this brings complications, the EDM measurements may also allow the only access to CP violation in the Hee, $Hu\bar{u}$, and $Hd\bar{d}$ interactions. Resolving all constraints simultaneously will require direct measurements of the H boson couplings in combination with EDM measurements. Moreover, it has not been experimentally established if the H boson couples to the first-family fermions. In case these couplings are absent or significantly suppressed, EDM measurements provide no constraints of CP violation in H boson interactions.

As part of this Snowmass study, we examine EDM constraints on parameters in Table I and add the Hee, $Hu\bar{u}$, and $Hd\bar{d}$ couplings in Table II. These constraints from the present EDM measurements are obtained in Appendix C. In Table II, only one CP-odd HX coupling is allowed to be present at a time. As it can also be seen in Fig. 6 of Appendix C, constraints on individual couplings $H\gamma\gamma$, $HZ\gamma$, HZZ are essentially lost if two other couplings are allowed to be present, but a big part of parameter space is still excluded from a correlated measurement. Most constraints on the parameters in Table II are dominated by the the current limit on electron EDM $d_e < 1.1 \times 10^{-29}\, e\,\text{cm}$ [128] from the ThO measurement, while the CP-odd Hgg, $Hu\bar{u}$, and $Hd\bar{d}$ couplings are constrained by the neutron [129] and mercury [130] EDMs. The limit on the neutron EDM is $d_n < 1.8 \times 10^{-26}\, e\,\text{cm}$ [129], and the mercury EDM constraint is equivalent to a similar limit on d_n [130], for the couplings under consideration here.

TABLE II: Constraints on the parameter $\left|\frac{f_{CP}^{HX}}{1-f_{CP}^{HX}}\right|$ at 68% C.L. from EDM measurements, assuming only one CP-odd HX coupling is nonzero at a time. Refer to Appendix C for more details.

HX coupling	Hgg	$H\gamma\gamma$	$HZ\gamma$	HZZ	$Ht\bar{t}$	$Hu\bar{u}$	$Hd\bar{d}$	$H\tau\tau$	$H\mu\mu$	Hee
$f_{CP}^{HX}/(1-f_{CP}^{HX}) <$	0.12	$2.4 \cdot 10^{-8}$	$4.4 \cdot 10^{-8}$	$1.2 \cdot 10^{-13}$	$4.3 \cdot 10^{-7}$	0.72	0.039	$2.2 \cdot 10^{-2}$	36	$1.1 \cdot 10^{-6}$

Over the next two decades, one could expect an order of magnitude increase in the precision of the electron EDM every 5-6 years, e.g. Fig. 5 in Ref. [122]. There is also a dramatic increase possible in the nucleon EDM measurements, e.g. Fig. 8 in Ref. [122]. There is a proposal to reach a precision on the proton EDM $d_p < 10^{-29}\, e\,\text{cm}$ using the proton storage ring within the next decade [131], which would be a big improvement over the current neutron EDM constraint. This may lead to an improvement by 10^3 in constraints on CP-odd Hgg, $Hu\bar{u}$, and $Hd\bar{d}$ couplings, and

potentially to an improvement by 10^6 in constraints on corresponding f_{CP}^{HX}. We note that even under the assumption of one CP-odd contribution to EDM, the expected constraint on f_{CP}^{Hgg} at the HL-LHC in Table I is stronger than the present EDM constraint in Table II. With the above potential improvement on the proton EDM using the proton storage ring, this will change. However, the HL-LHC constraints will be essential in order to analyze all CP-violating couplings in Table II without assumptions that only one CP-odd coupling is nonzero at a time.

IX. SUMMARY

The search for CP violation is an important research direction of future experiments in particle physics, as CP violation is required for baryogengesis and cannot be sufficiently explained with present knowledge. We have reviewed the status and prospects of the search for CP violation in interactions of the Higgs boson (H) with either fermions or bosons at the current and future proposed facilities. The dedicated CP-sensitive measurements of the H boson provide simple but reliable benchmarks that can serve as a guide to compare future facilities as part of the Particle Physics Community Planning Exercise (a.k.a. "Snowmass"). These benchmarks are compared between proton, electron-positron, photon, and muon colliders in Table I.

Hadron colliders provide essentially the full spectrum of possible measurements sensitive to CP violation in the H boson interactions accessible in the collider experiments, with the exception of interactions with light fermions, such as $H\mu\mu$. The CP structure of the H boson couplings to gluons cannot be easily measured at a lepton collider, because the decay to two gluons does not allow easy access to gluon polarization. On the other hand, most other processes could be studied at an e^+e^- collider, especially with the beam energy above the $t\bar{t}H$ threshold. Future e^+e^- colliders are expected to provide comparable CP sensitivity to HL-LHC in Hff couplings, such as $Ht\bar{t}$ and $H\tau\tau$, and HZZ/HWW couplings.

A muon collider operating at the H boson pole gives access to CP structure of the $H\mu\mu$ vertex using the beam polarization. It is not possible to study the CP structure in the decay because the muon polarization is not accessible. At a muon collider operating both at the H boson pole and at higher energy, analysis of the H boson decays is also possible. However, this analysis is similar to the studies performed at other facilities and depends critically on the number of the H bosons produced and their purity. A photon collider operating at the H boson pole allows measurement of the CP structure of the $H\gamma\gamma$ vertex using the beam polarization. Otherwise, the measurement of CP in both $H\gamma\gamma$ and $HZ\gamma$ interactions is challenging and requires high statistics of H boson decays with virtual photons, which would require a production rate beyond that of the HL-LHC for sensitive measurements.

Measurements of the electric dipole moments of atoms and molecules set stringent constraints on CP-violating interactions beyond the SM appearing in loop calculations. Assuming only one CP-odd H boson coupling is nonzero at a time, EDM constraints can be interpreted as limits on CP violation in the H boson interactions, as shown in Table II. Such constraints are either tighter or expected to be tighter with EDM measurements projected in the next two decades when compared to CP violation measurements in direct H boson interactions at colliders. However, resolving all constraints simultaneously will require direct measurements of the H boson couplings in combination with EDM measurements. Moreover, it has not been experimentally established whether the H boson couples to the first-family fermions, and if such couplings are absent or suppressed, EDM measurements provide no constraints of CP violation in H boson interactions.

In the end, we conclude that the various collider and low-energy experiments provide complementary CP-sensitive measurements of the H boson interactions. The HL-LHC provides the widest spectrum of direct measurements in the H boson interactions and is unique in measuring couplings to gluons, but it lacks the ability to set precise constraints on interactions with photons and muons. Such constraints may become possible with either photon or muon colliders operating at the H boson pole. The electron-positron collider may allow constraints similar to HL-LHC in couplings to fermions and heavy weak bosons. Given the coverage provided by HL-LHC, we expect that a future pp collider, such as FCC-hh or SPPC, will surpass HL-LHC and allow the furthest reach in CP-sensitive measurements of the H boson interactions among the collider experiments.

Acknowledgments: We would like to thank all contributors of individual studies and participants of the "Snowmass" community exercise. A.V.G., J.D., L.S.M.G., and S.K. thank the United States National Science Foundation for the financial support, under grant number PHY-2012584. R.K.B and D.G. thank the United States Department of Energy for the financial support, under grant number DE-SC0016013.

Appendix A: Recent updates of the studies at a hadron collider

Contributed by Jeffrey Davis, Savvas Kyriacou, and Jeffrey Roskes.

In this Section, we update the feasibility study of the CP-odd $H\gamma\gamma$ and $HZ\gamma$ interactions at the HL-LHC, which is documented in Ref. [71], in order to adopt the $f_{CP}^{HV\gamma}$ benchmark parameters introduced in Eq. (2). As discussed in Sections III and V B, it is not possible to study the CP structure of the $H\gamma\gamma$ and $HZ\gamma$ couplings in the $H \to \gamma\gamma$ and $H \to Z\gamma$ decays. The rates of these decays put constraints on the quadrature sum of the CP-odd and CP-even couplings, which can be parameterized, following the notation in Eq. (1) and in Ref. [71], as

$$\mathrm{g}^{\mathrm{eff}\ 2}_{HV\gamma} \equiv \frac{\Gamma_{H\to V\gamma}}{\Gamma^{\mathrm{SM}}_{H\to V\gamma}} \simeq \frac{1}{\left(a_2^{V\gamma,\mathrm{SM}}\right)^2}\left[\left(a_2^{V\gamma,\mathrm{SM}} + a_2^{V\gamma}\right)^2 + \left(a_3^{V\gamma}\right)^2\right], \tag{A1}$$

where $V = Z$ or γ and $a_2^{\gamma\gamma,\mathrm{SM}} = 0.00423$ and $a_2^{Z\gamma,\mathrm{SM}} = 0.00675$ are the effective values of the point-like CP-even couplings generated by SM loops with the W boson and charged fermions. In this parameterization, the SM corresponds to $(a_2^{\gamma\gamma}, a_3^{\gamma\gamma}) = (0,0)$ and $(a_2^{Z\gamma}, a_3^{Z\gamma}) = (0,0)$.

The constraints on $(a_2^{\gamma\gamma}, a_3^{\gamma\gamma})$ and $(a_2^{Z\gamma}, a_3^{Z\gamma})$ from the HL-LHC measurements of the $H \to \gamma\gamma$ and $H \to Z\gamma$ decay rates, assuming that production rates can be constrained in the global analysis of the H boson data to a good enough precision, appear as circles on the 2D planes, as indicated in Fig. 3. These circles correspond to the fixed values of $\mathrm{g}^{\mathrm{eff}}_{HV\gamma}$ in Eq. (A1). The centers of the circles are at $(-a_2^{V\gamma,\mathrm{SM}}, 0)$. All points on a circle of a given radius have equal probability, and rotation around the circle can be parameterized with the $f_{CP}^{HV\gamma}$ value, as indicated on the graphs in Fig. 3. With the $H \to \gamma\gamma$ and $H \to Z\gamma$ decay rates only, the $f_{CP}^{HV\gamma}$ values are not constrained.

It has been demonstrated in Ref. [71] that the data from $H \to 4\ell$, VBF, and VH can resolve the points along the circles on the $(a_2^{V\gamma}, a_3^{V\gamma})$ plane. While the VBF and VH channels do provide information to differentiate the CP-odd and CP-even couplings, the dominant precision comes from the $H \to ZZ/Z\gamma^*/\gamma^*\gamma^* \to 4\ell$ process, and we refer to Ref. [71] for an explanation of this effect. A 68% C.L. exclusion of $f_{CP}^{H\gamma\gamma} = 0.5$ can be achieved with 3,000 fb^{-1} (left plot in Fig. 3), while $f_{CP}^{HZ\gamma} = 1.0$ can be excluded with 5,000 fb^{-1} (right plot in Fig. 3). We take these as estimates of the HL-LHC precision on $f_{CP}^{H\gamma\gamma}$ and $f_{CP}^{HZ\gamma}$, but note that a more detailed study and incorporation of multiple production channels may improve this further.

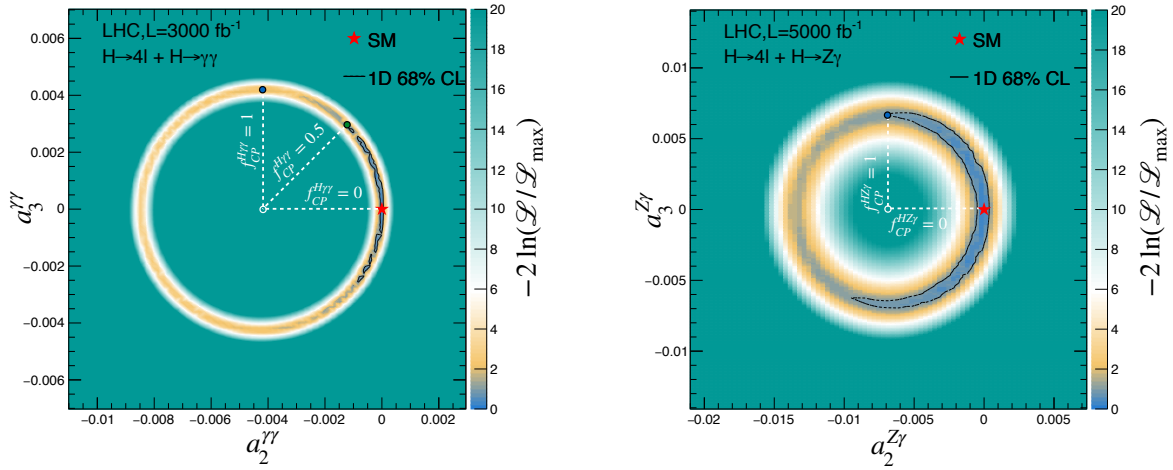


FIG. 3: Expected two-dimensional constraints on $(a_2^{\gamma\gamma}, a_3^{\gamma\gamma})$ (left), and $(a_2^{Z\gamma}, a_3^{Z\gamma})$ (right) using Eq. (A1) and the HL-LHC projection of analysis of the $H \to \gamma\gamma$, $H \to Z\gamma$, $H \to 4\ell$, VBF, and VH channels with 3,000 fb^{-1} (left) and 5,000 fb^{-1} (right) following the study from Ref. [71].

Appendix B: Recent updates of the studies at an electron-positron collider

Contributed by Lucas S. Mandacarú Guerra and Savvas Kyriacou.

In this Section, we present a feasibility study of the CP-odd $H\gamma\gamma$ and $HZ\gamma$ interactions at an e^+e^- machine and revise the study of the CP-odd HZZ interactions documented in Snowmass-2013 writeup [76] and Ref. [52]. We start with the study of the $e^+e^- \to VH$ production at $\sqrt{s} = 250\,\text{GeV}$ and $250\,\text{fb}^{-1}$, with $H \to b\bar{b}$ and $V \to \ell\ell$. We note that with the $H\gamma\gamma$ and $HZ\gamma$ couplings, both $V = Z$ and γ^* are possible. The dominant contribution comes from the SM HZZ couplings, and in Ref. [52] it is estimated that about 1870 events would be reconstructed. The dominant background is modeled with the process $e^+e^- \to ZZ/Z\gamma^* \to b\bar{b}\ell\ell$. The analysis is based on the 4D parameterization of the mass-angular distributions $(m_{\ell\ell}, \cos\theta_1, \cos\theta_2, \Phi)$ and otherwise follows a similar technique to that employed in HL-LHC studies in Appendix A.

First, we reproduce the feasibility study of the f_{CP}^{HZZ} parameter and find results consistent with those reported in Ref. [52]. The expected constraints at four energy and luminosity scenarios are shown in Table III and the likelihood scans are shown in Fig. 4. In addition, we present expected constraints with luminosity ten times larger than that

TABLE III: List of expected precision (at 68% C.L.) of CP-sensitive measurements of the parameter f_{CP}^{HVV} defined in Eq. (6) in the process $e^+e^- \to Z^* \to ZH \to \ell\ell b\bar{b}$ in several energy and luminosity scenarios. Also shown are expected constraints (at 68% C.L.) on the $f^{V\gamma}$ parameters in the same process, which are expressed as fractions of the $a_2^{V\gamma}$ and $a_3^{V\gamma}$ contributions combined in the $H \to 2e2\mu$ decay cross sections, where the most likely values of $f^{\gamma\gamma} = 0.0016$ and $f^{Z\gamma} = 0.0050$ were generated, corresponding to $a_2^{\gamma\gamma,\text{SM}}$ and $a_2^{Z\gamma,\text{SM}}$. Only the $f_{CP}^{Z\gamma}$ parameter in the last energy and luminosity scenario allows a non-trivial constraint at 68% C.L., as indicated in the last column.

E (GeV)	$\mathcal{L}$ (fb^{-1})	f_{CP}^{HVV}	$f^{\gamma\gamma}$	$f^{Z\gamma}$	$f_{CP}^{\gamma\gamma}$	$f_{CP}^{Z\gamma}$
250	250	$\pm 3.4\cdot10^{-4}$	< 0.144	< 0.234	–	–
250	2,500	$\pm 3.9\cdot10^{-5}$	< 0.037	< 0.079	–	–
350	350	$\pm 1.2\cdot10^{-4}$	< 0.058	< 0.088	–	–
350	3,500	$\pm 2.9\cdot10^{-5}$	< 0.016	< 0.032	–	–
500	500	$\pm 4.3\cdot10^{-5}$	< 0.028	< 0.039	–	–
500	5,000	$\pm 1.3\cdot10^{-5}$	< 0.009	< 0.016	–	–
1,000	1,000	$\pm 1.0\cdot10^{-5}$	< 0.009	< 0.014	–	–
1,000	10,000	$\pm 3.0\cdot10^{-6}$	< 0.004	$0.0050^{+0.0026}_{-0.0028}$	–	± 0.96

considered in Snowmass-2013 studies, which is consistent within a factor of two with the more recent collider scenarios considered in Snowmass-2022 studies, as outlined in Ref. [80]. This indicates that the scaling with luminosity is close to linear at the lower energy scenario, while it is in between the linear and square root at higher energies. This luminosity dependence can also be seen in Fig. 4. The new expectation at 250 GeV is about a factor of 2 tighter than that obtained for Snowmass-2013 [52, 76]. However, the previous expected constrains at 68% C.L. were obtained the assumption of a non-zero CP violation near the threshold of discovery. The new constraints are obtained under the assumption of null CP violation, to be consistent with other studies performed since then. The differences at other energies are even smaller. We also take our study one step further and obtained constraints in two ways: with all other CP-even couplings (with the exception of the tree-level SM coupling, which is always left unconstrained) either constrained to zero, as expected in the SM, or left unconstrained in the fit. The list of CP-even couplings can be found in Eq. (5) and includes a_1^{HZZ}, a_2^{HZZ}, and two other couplings κ_1^{HZZ} and $\kappa_2^{HZ\gamma}$, which correspond to the higher-order q^2 terms in expansion of a_1^{HVV}. The expected constraints in Table III do not differ within quoted precision either with or without the CP-even anomalous couplings floated in the fit.

Then, we turn to the prospect of the $(a_2^{\gamma\gamma}, a_3^{\gamma\gamma})$ and $(a_2^{Z\gamma}, a_3^{Z\gamma})$ measurements in the $e^+e^- \to VH$ production. We can already point out that using the $a_2^{\gamma\gamma,\text{SM}}$ and $a_2^{Z\gamma,\text{SM}}$ values, quoted in Appendix A, one can expect only about 0.1 and 2 events, respectively, if these are the only contributions to the HVV production amplitude in the process $e^+e^- \to Z^* \to ZH \to \ell\ell b\bar{b}$ at $\sqrt{s} = 250\,\text{GeV}$ and $250\,\text{fb}^{-1}$. With such a small contribution, it is not feasible to expect strong constraints on the photon couplings. Nonetheless, the full study with the 4D likelihood fit is essential to take into account the effects of interference of the photon couplings with the dominant SM tree-level HZZ contribution. This interference is not very strong in the case of the $H\gamma\gamma$ couplings due to very different $m_{\ell\ell}$ spectra. We parameterize the $a_2^{\gamma\gamma}, a_3^{\gamma\gamma}, a_2^{Z\gamma}, a_3^{Z\gamma}$ contributions in terms of four parameters: two fractions $f^{\gamma\gamma}$ and $f^{Z\gamma}$, expressed as the $a_2^{V\gamma}$

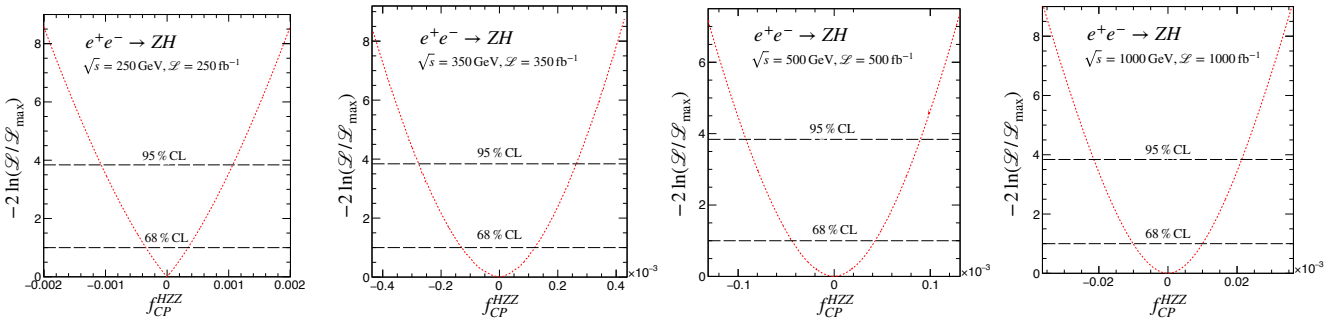


FIG. 4: Expected constraints on the f_{CP}^{HVV} parameter in the process $e^+e^- \to Z^* \to ZH \to \ell\ell b\bar{b}$ at four energy and luminosity scenarios.

and $a_3^{V\gamma}$ contributions combined in the $H \to 2e2\mu$ decay cross sections, and two $f_{CP}^{\gamma\gamma}$ and $f_{CP}^{Z\gamma}$ parameters defined in Eq. (2) for $H \to V\gamma$. Examples of the fits for $f^{\gamma\gamma}$ and $f^{Z\gamma}$ are shown in Fig. 5, and expected upper limits in eight scenarios are shown in Table III. We conclude that there is not enough sensitivity to isolate the $H\gamma\gamma$ and $HZ\gamma$ contributions with the rates generated by the $a_2^{\gamma\gamma,\text{SM}}$ and $a_2^{Z\gamma,\text{SM}}$ couplings. Therefore, constraints on $f_{CP}^{HZ\gamma}$ and $f_{CP}^{H\gamma\gamma}$ are not feasible if these contributions are comparable to the SM expectation. Only the $f_{CP}^{Z\gamma}$ parameter at $\text{E} = 1\,\text{TeV}$ and $\mathcal{L} = 10\,\text{ab}^{-1}$ allows a non-trivial constraint at 68% C.L., as indicated in the last column of Table III, but still with essentially 100% uncertainties. Of course, should there be anomalously large $f^{\gamma\gamma}$ or $f^{Z\gamma}$, one could isolate CP-odd contributions with a relatively high precision, but such a scenario is excluded by the rates of the $H \to \gamma\gamma$ or $H \to Z\gamma$ processes. Nonetheless, we note that one will start approaching sensitivity to the SM rate faster with the higher-energy collider scenarios, as indicated in Table III.

Expected constraints presented in Table III assume no beam polarization in e^+e^- collisions. At a linear collider, $(+80\%, -30\%)$ polarization of the (e^-, e^+) beams is proposed, which may further improve precision of certain measurements [80]. Therefore, we have repeated the feasibility study in Table III with such polarization. Generally, there are improvements mainly because the cross section of the background process $e^+e^- \to ZZ/Z\gamma^* \to b\bar{b}\ell\ell$ is reduced (by approximately 30%), while cross sections of the signal VH processes generated by the HZZ, $HZ\gamma$, and $H\gamma\gamma$ couplings are increased (by approximately 8%, 22%, and 24%, respectively). However, the small, positive interference between the amplitudes generated by the a_1^{ZZ} and $a_2^{Z\gamma}$ couplings with unpolarized beams becomes large and negative with the beam polarization, which may compensate for such an effect in the measurement of the $f^{Z\gamma}$ parameter. Such large negative interference with beam polarization is stronger at lower energies. With beam polarization, we find less than 10% improvement in expected constraints on f_{CP}^{HZZ} quoted in Table III. While we see larger variation in expected constraints on $f^{\gamma\gamma}$ and $f^{Z\gamma}$, due to the above effects, the picture remains qualitatively the same. For example, the expected constraint on $f_{CP}^{Z\gamma}$ at 68% C.L. is improved by 12% in the $\text{E} = 1\,\text{TeV}$ and $\mathcal{L} = 10\,\text{ab}^{-1}$ scenario.

While we have not performed a study of the CP-odd $H\gamma\gamma$ and $HZ\gamma$ interactions in VBF production $e^+e^- \to$

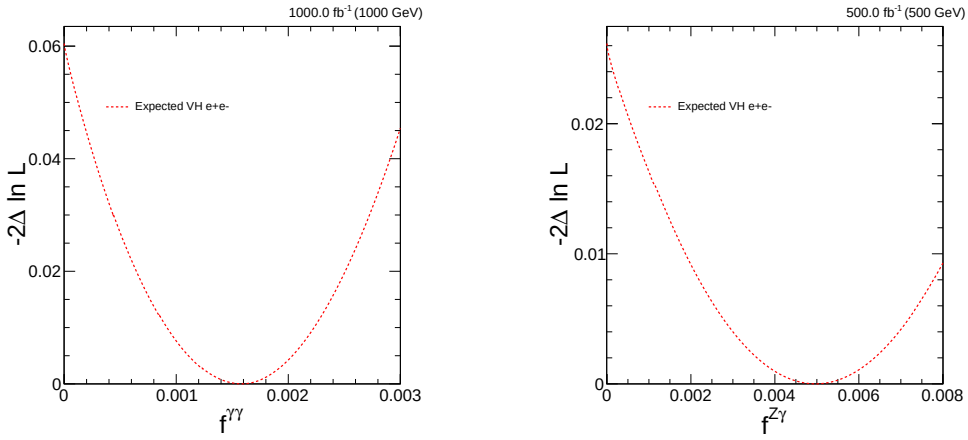


FIG. 5: Examples from Table III of expected constraints on the $f^{V\gamma}$ parameters, where the most likely values are $f^{\gamma\gamma} = 0.0016$ and $f^{Z\gamma} = 0.0050$, in the $e^+e^- \to Z^* \to ZH \to \ell\ell b\bar{b}$ process in two energy and luminosity scenarios.

$e^+e^-(ZZ/Z\gamma^*/\gamma^*\gamma^*) \to e^+e^-H$, we expect a conclusion similar to that in $e^+e^- \to VH$ by analogy with the HL-LHC studies in Appendix A and Ref. [71]. In the latter study, it was found that the $H \to ZZ/Z\gamma^*/\gamma^*\gamma^* \to 4\ell$ decay process is more powerful in constraining the photon couplings than both the VBF and VH processes, because the preferred range of q^2 in these processes leads to the γ^* going far off-shell. This is the reverse of the situation with the HZZ couplings, which are better constrained in production, and where an increase in the collider energy $\sqrt{s}$ brings a benefit. It is possible to study the $H \to 4\ell$ process in the e^+e^- production, but the expected number of events is only about 7 at $\sqrt{s} = 250\,\text{GeV}$ and $250\,\text{fb}^{-1}$, which is too small for a study. In a clean e^+e^- environment, one could consider the hadronic decays of the Z bosons in the $H \to ZZ$ process, but the full number of $H \to ZZ$ events of about 1600 is still much smaller than the expected number of $H \to 4\ell$ events at the HL-LHC. We make a preliminary conclusion that most likely it will not be feasible to constrain the CP-odd photon couplings $a_3^{V\gamma}$ of the H boson with a precision comparable to the CP-even contribution to the decay process $a_2^{V\gamma,\text{SM}}$ at an e^+e^- collider with parameters outlined in Table I. Nonetheless, we encourage a dedicated study of the VBF process to confirm this expectation.

Appendix C: EDM constraints

Contributed by Wouter Dekens.

The CP-odd Higgs couplings not only appear in processes directly involving the Higgs boson, but also affect low-energy precision experiments through loop diagrams. Measurements of the EDMs of the neutron [129], mercury [130], and the ThO molecule [128] set particularly stringent constraints on CP-violating interactions beyond the SM. The loop contributions to these observables have been widely considered in the context of the SMEFT, see e.g. Refs. [126, 132–136]. In these analyses, the CP-violating SMEFT interactions are first matched onto a low-energy theory in which the heavy SM degrees of freedom have been integrated out and subsequently evolved to the QCD scale. At this scale the quark-level theory can be matched to Chiral perturbation theory, giving rise to a description in terms of CP-odd interactions between hadrons, photons, and electrons, which can then be used to compute the EDMs of nucleons, atoms, and molecules.

The couplings of the Higgs to gauge bosons induce the (chromo) electric dipole moments of fermions through one-loop diagrams [135–137], while the couplings to t, τ, and μ contribute through two-loop Barr-Zee graphs [138]. For almost all of the couplings the most relevant contributions are those to the electron EDM, which is very stringently constrained by the ThO measurement. The exception is $f_{CP}^{H\text{gg}}$, which does not induce the electron EDM and gives rise to the EDMs of the neutron and mercury instead. These different contributions have been evaluated in the SMEFT in Refs. [126] and [133] for the Higgs-gauge (f_{CP}^{HVV}) and Higgs-fermion (f_{CP}^{Hff}) couplings, respectively. In this language, the f_{CP}^{HVV} and f_{CP}^{Hff} couplings correspond to the Wilson coefficients of dimension-six operators in the Warsaw basis [139, 140],

$$\begin{pmatrix} \sqrt{r_{H\text{gg}}} \\ \sqrt{r_{H\gamma\gamma}} \\ \sqrt{r_{HZ\gamma}} \\ \sqrt{r_{HZZ}} \end{pmatrix} = \begin{pmatrix} \frac{12\pi}{\alpha_s} & 0 & 0 & 0 \\ 0 & -410 & -120 & 220 \\ 0 & 130 & -130 & 82 \\ 0 & 0.082 & 0.28 & 0.15 \end{pmatrix} \cdot \begin{pmatrix} v^2 C_{H\tilde{G}} \\ v^2 C_{H\tilde{B}} \\ v^2 C_{H\tilde{W}} \\ v^2 C_{H\tilde{W}B} \end{pmatrix},$$

$$\sqrt{r_{Htt}} = \frac{v^2 \text{Im}\, C_{uH}^{(33)}}{y_t}, \quad \sqrt{r_{Huu}} = \frac{v^2 \text{Im}\, C_{uH}^{(11)}}{y_u}, \quad \sqrt{r_{Hdd}} = \frac{v^2 \text{Im}\, C_{dH}^{(11)}}{y_d},$$

$$\sqrt{r_{H\tau\tau}} = \frac{v^2 \text{Im}\, C_{eH}^{(33)}}{y_\tau}, \quad \sqrt{r_{H\mu\mu}} = \frac{v^2 \text{Im}\, C_{eH}^{(22)}}{y_\mu}, \quad \sqrt{r_{Hee}} = \frac{v^2 \text{Im}\, C_{eH}^{(11)}}{y_e},$$

where $r_X = \frac{f_{CP}^X}{1 - f_{CP}^X}$, $y_f = \sqrt{2} m_f / v$, v is the Higgs vacuum expectation value $v \simeq 246$ GeV, and we used the tree-level results of Ref. [141] to evaluate $\Gamma_{H\to VV'}^{CP\,\text{odd}}$. Note that since the f_{CP}^{HX} are defined through the decay rates, there is a sign ambiguity for each of the $\sqrt{f_{CH}^{HX}}$.

Using the above relations, the analyses of Refs. [126] and [133] can be rephrased in terms of f_{CP}^{HVV} and f_{CP}^{Hff}, respectively. The resulting limits, assuming only one of of the couplings is nonzero at a time, are shown in Table II. The limits are dominated by the ThO measurement for all couplings apart from $f_{CP}^{H\text{gg}}$, f_{CP}^{Huu}, and f_{CP}^{Hdd}, which do not induce an electron EDM and only contribute to the neutron and mercury EDMs. Although the theoretical uncertainties related to the interpretation of the ThO measurement are small, there are significant uncertainties related to the hadronic and nuclear matrix elements that appear in the expressions for the neutron and mercury EDMs, see Refs. [142, 143] for an overview. The table shows the constraints on the Huu, Hdd, and $H\text{gg}$ couplings

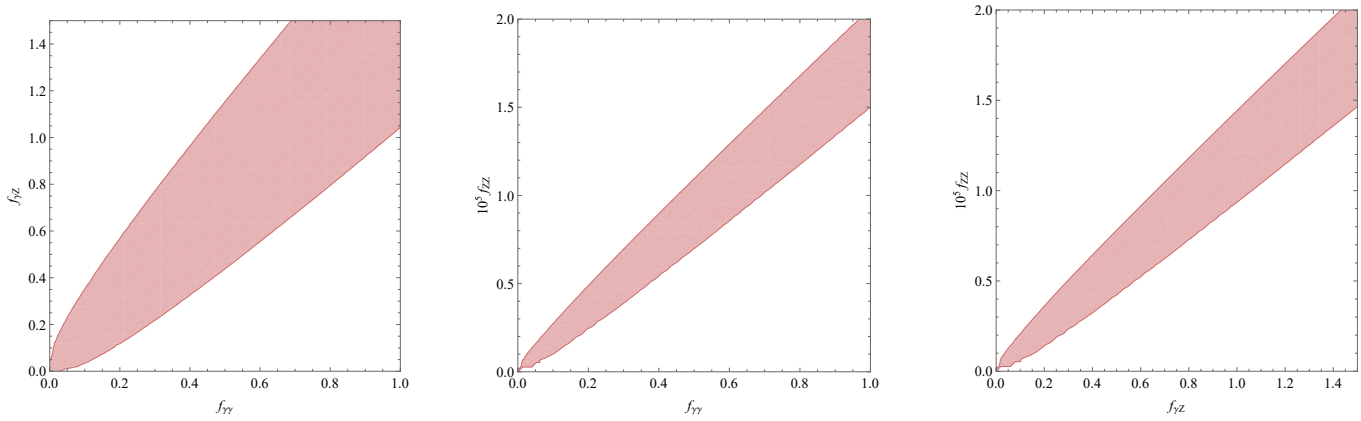


FIG. 6: The red shaded regions depict the parameter space allowed by EDM measurements at 90% C.L. assuming that the $f_{CP}^{H\gamma\gamma}$, $f_{CP}^{HZ\gamma}$, and f_{CP}^{HZZ} couplings are nonzero simultaneously.

that results from varying these matrix elements within their allowed ranges, corresponding to the 'Rfit' approach of Ref. [126]. In this case the dominant constraint arises from the neutron EDM. If one instead sets the matrix elements to their central values, the limits on f_{CP}^{Hgg} and f_{CP}^{Huu} (f_{CP}^{Hdd}) improve by a factor of $\sim 10^3$ (10^2). The most stringent limits on the Yukawa couplings are then set by the mercury EDM, while the constraints on f_{CP}^{Hgg} from the neutron and mercury EDMs are comparable. The bounds in Table II are more stringent than those in Table I by several orders of magnitude for the couplings of the Higgs boson to electroweak gauge bosons and the top quark. In contrast, for f_{CP}^{Hgg} and $f_{CP}^{H\tau\tau}$, the sensitivity of the 14 TeV LHC is comparable to the EDM constraints.

Although some of the limits in Table II are more stringent than the projections in Table I, they do assume that only one of the couplings is turned on at a time. However, most beyond-the-SM scenarios induce multiple operator coefficients, motivating analyses of scenarios in which several operators nonzero. As an example, we consider the case in which the three Higgs couplings to electroweak gauge bosons, $f_{CP}^{H\gamma\gamma}$ $f_{CP}^{HZ\gamma}$, and f_{CP}^{HZZ}, are present, with the remaining couplings set to zero. Although we in principle have measurements of the EDMs of three different systems, it turns out that they do not give enough information to constrain all three couplings, see Ref. [126] for details. As a result, there is one unconstrained linear combination of the three couplings, corresponding to a tuning of the coefficients such that the contributions to EDMs cancel. The allowed parameter space in this scenario is depicted in Fig. 6, where each panel shows the allowed values for two of the couplings while marginalizing over the remaining coefficient. Clearly, the couplings are allowed to be much larger than in the single-coupling analysis, in part due to the unconstrained linear combination. Nevertheless, as can be seen from Fig. 6, there is still a significant part of parameter space that can be excluded by EDM measurements, especially taking into account that each allowed point in these figures requires a precisely tuned value of the third coupling in order to cancel significant contributions to EDMs.

[1] A. D. Sakharov, "Violation of CP Invariance, C asymmetry, and baryon asymmetry of the universe", *Pisma Zh. Eksp. Teor. Fiz.* **5** (1967) 32–35, doi:10.1070/PU1991v034n05ABEH002497.

[2] M. Kobayashi and T. Maskawa, "CP Violation in the Renormalizable Theory of Weak Interaction", *Prog. Theor. Phys.* **49** (1973) 652–657, doi:10.1143/PTP.49.652.

[3] M. E. Shaposhnikov, "Baryon Asymmetry of the Universe in Standard Electroweak Theory", *Nucl. Phys. B* **287** (1987) 757–775, doi:10.1016/0550-3213(87)90127-1.

[4] CMS Collaboration, "Study of the mass and spin-parity of the Higgs boson candidate via its decays to Z boson pairs", *Phys. Rev. Lett.* **110** (2013) 081803, doi:10.1103/PhysRevLett.110.081803, arXiv:1212.6639.

[5] ATLAS Collaboration, "Evidence for the spin-0 nature of the Higgs boson using ATLAS data", *Phys. Lett.* **B726** (2013) 120–144, doi:10.1016/j.physletb.2013.08.026, arXiv:1307.1432.

[6] CMS Collaboration, "Measurement of the properties of a Higgs boson in the four-lepton final state", *Phys. Rev.* **D89** (2014) 092007, doi:10.1103/PhysRevD.89.092007, arXiv:1312.5353.

[7] CMS Collaboration, "Constraints on the spin-parity and anomalous HVV couplings of the Higgs boson in proton collisions at 7 and 8 TeV", *Phys. Rev.* **D92** (2015) 012004, doi:10.1103/PhysRevD.92.012004, arXiv:1411.3441.

[8] ATLAS Collaboration, "Study of the spin and parity of the Higgs boson in diboson decays with the ATLAS detector", *Eur. Phys. J.* **C75** (2015) 476, doi:10.1140/epjc/s10052-015-3685-1, arXiv:1506.05669.

[9] CMS Collaboration, "Combined search for anomalous pseudoscalar HVV couplings in VH(H $\to$ b$\bar{\text{b}}$) production and H $\to$ VV decay", *Phys. Lett. B* **759** (2016) 672, doi:10.1016/j.physletb.2016.06.004, arXiv:1602.04305.

[10] ATLAS Collaboration, "Test of CP invariance in vector-boson fusion production of the Higgs boson using the Optimal Observable method in the ditau decay channel with the ATLAS detector", *Eur. Phys. J. C* **76** (2016) 658, doi:10.1140/epjc/s10052-016-4499-5, arXiv:1602.04516.

[11] CMS Collaboration, "Constraints on anomalous Higgs boson couplings using production and decay information in the four-lepton final state", *Phys. Lett. B* **775** (2017) 1, doi:10.1016/j.physletb.2017.10.021, arXiv:1707.00541.

[12] ATLAS Collaboration, "Measurement of inclusive and differential cross sections in the $H \to ZZ^* \to 4\ell$ decay channel in pp collisions at $\sqrt{s} = 13$ TeV with the ATLAS detector", *JHEP* **10** (2017) 132, doi:10.1007/JHEP10(2017)132, arXiv:1708.02810.

[13] ATLAS Collaboration, "Measurement of the Higgs boson coupling properties in the $H \to ZZ^* \to 4\ell$ decay channel at $\sqrt{s} = 13$ TeV with the ATLAS detector", *JHEP* **03** (2018) 095, doi:10.1007/JHEP03(2018)095, arXiv:1712.02304.

[14] ATLAS Collaboration, "Measurements of Higgs boson properties in the diphoton decay channel with 36 fb^{-1} of pp collision data at $\sqrt{s} = 13$ TeV with the ATLAS detector", *Phys. Rev. D* **98** (2018) 052005, doi:10.1103/PhysRevD.98.052005, arXiv:1802.04146.

[15] CMS Collaboration, "Measurements of the Higgs boson width and anomalous HVV couplings from on-shell and off-shell production in the four-lepton final state", *Phys. Rev.* **D99** (2019) 112003, doi:10.1103/PhysRevD.99.112003, arXiv:1901.00174.

[16] CMS Collaboration, "Constraints on anomalous HVV couplings from the production of Higgs bosons decaying to τ lepton pairs", *Phys. Rev. D* **100** (2019) 112002, doi:10.1103/PhysRevD.100.112002, arXiv:1903.06973.

[17] CMS Collaboration, "Measurements of t$\bar{\text{t}}H$ Production and the CP Structure of the Yukawa Interaction between the Higgs Boson and Top Quark in the Diphoton Decay Channel", *Phys. Rev. Lett.* **125** (2020) 061801, doi:10.1103/PhysRevLett.125.061801, arXiv:2003.10866.

[18] ATLAS Collaboration, "CP Properties of Higgs Boson Interactions with Top Quarks in the $t\bar{t}H$ and tH Processes Using $H \to \gamma\gamma$ with the ATLAS Detector", *Phys. Rev. Lett.* **125** (2020), no. 6, 061802, doi:10.1103/PhysRevLett.125.061802, arXiv:2004.04545.

[19] ATLAS Collaboration, "Test of CP invariance in vector-boson fusion production of the Higgs boson in the H $\to \tau\tau$ channel in proton$-$proton collisions at $\sqrt{s} = 13$ TeV with the ATLAS detector", *Phys. Lett. B* **805** (2020) 135426, doi:10.1016/j.physletb.2020.135426, arXiv:2002.05315.

[20] CMS Collaboration, "Constraints on anomalous Higgs boson couplings to vector bosons and fermions in its production and decay using the four-lepton final state", *Phys. Rev. D* **104** (2021), no. 5, 052004, doi:10.1103/PhysRevD.104.052004, arXiv:2104.12152.

[21] CMS Collaboration, "Analysis of the CP structure of the Yukawa coupling between the Higgs boson and τ leptons in proton-proton collisions at $\sqrt{s} = 13$ TeV", arXiv:2110.04836.

[22] ATLAS Collaboration, "Constraints on Higgs boson properties using $WW^*(\to e\nu\mu\nu)jj$ production in 36.1 fb^{-1} of $\sqrt{s}$=13 TeV pp collisions with the ATLAS detector", arXiv:2109.13808.

[23] CMS Collaboration, "Measurement of the Higgs boson width and evidence of its off-shell contributions to ZZ production", *Nat. Phys.* **18** (2022) 1329, doi:10.1038/s41567-022-01682-0, arXiv:2202.06923.

[24] CMS Collaboration, "Constraints on anomalous Higgs boson couplings to vector bosons and fermions from the production of Higgs bosons using the $\tau\tau$ final state", arXiv:2205.05120.

[25] CMS Collaboration, "Search for CP violation in $t\bar{t}H$ and tH production in multilepton channels at $\sqrt{s} = 13\,\text{TeV}$",. https://cds.cern.ch/record/2803420.

[26] ATLAS Collaboration, "Probing the CP nature of the top-Higgs Yukawa coupling in $t\bar{t}H$ and tH events with $H \to b\bar{b}$ at the LHC",. https://cds.cern.ch/record/2805772.

[27] ATLAS Collaboration, "Measuring CP properties of Higgs boson interactions with τ leptons with the ATLAS detector",. https://cds.cern.ch/record/2809728.

[28] C. A. Nelson, "Correlation between decay planes in Higgs-boson decays into a W Pair (into a Z Pair)", *Phys. Rev. D* **37** (1988) 1220, doi:10.1103/PhysRevD.37.1220.

[29] A. Soni and R. M. Xu, "Probing CP violation via Higgs decays to four leptons", *Phys. Rev. D* **48** (1993) 5259, doi:10.1103/PhysRevD.48.5259, arXiv:hep-ph/9301225.

[30] D. Chang, W.-Y. Keung, and I. Phillips, "CP odd correlation in the decay of neutral Higgs boson into ZZ, W$^+$W$^-$, or t$\bar{\text{t}}$", *Phys. Rev. D* **48** (1993) 3225, doi:10.1103/PhysRevD.48.3225, arXiv:hep-ph/9303226.

[31] V. D. Barger et al., "Higgs bosons: Intermediate mass range at e+ e- colliders", *Phys. Rev. D* **49** (1994) 79, doi:10.1103/PhysRevD.49.79, arXiv:hep-ph/9306270.

[32] T. Arens and L. M. Sehgal, "Energy spectra and energy correlations in the decay $H \to ZZ \to \mu^+\mu^-\mu^+\mu^-$", *Z. Phys. C* **66** (1995) 89, doi:10.1007/BF01496583, arXiv:hep-ph/9409396.

[33] S. Bar-Shalom et al., "Large tree level CP violation in $e^+e^- \to t\bar{t}H^0$ in the two Higgs doublet model", *Phys. Rev. D* **53** (1996) 1162, doi:10.1103/PhysRevD.53.1162, arXiv:hep-ph/9508314.

[34] J. F. Gunion and X.-G. He, "Determining the CP nature of a neutral Higgs boson at the LHC", *Phys. Rev. Lett.* **76** (1996) 4468, doi:10.1103/PhysRevLett.76.4468, arXiv:hep-ph/9602226.

[35] T. Han and J. Jiang, "CP violating ZH coupling at e^+e^- linear colliders", *Phys. Rev. D* **63** (2001) 096007, doi:10.1103/PhysRevD.63.096007, arXiv:hep-ph/0011271.

[36] T. Plehn, D. L. Rainwater, and D. Zeppenfeld, "Determining the structure of Higgs couplings at the LHC", *Phys. Rev. Lett.* **88** (2002) 051801, doi:10.1103/PhysRevLett.88.051801, arXiv:hep-ph/0105325.

[37] S. Y. Choi, D. J. Miller, M. M. Mühlleitner, and P. M. Zerwas, "Identifying the Higgs spin and parity in decays to Z pairs", *Phys. Lett. B* **553** (2003) 61, doi:10.1016/S0370-2693(02)03191-X, arXiv:hep-ph/0210077.

[38] C. P. Buszello, I. Fleck, P. Marquard, and J. J. van der Bij, "Prospective analysis of spin- and CP-sensitive variables in $H \to ZZ \to \ell_1^+\ell_1^-\ell_2^+\ell_2^-$ at the LHC", *Eur. Phys. J. C* **32** (2004) 209, doi:10.1140/epjc/s2003-01392-0, arXiv:hep-ph/0212396.

[39] V. Hankele, G. Klamke, D. Zeppenfeld, and T. Figy, "Anomalous Higgs boson couplings in vector boson fusion at the CERN LHC", *Phys. Rev. D* **74** (2006) 095001, doi:10.1103/PhysRevD.74.095001, arXiv:hep-ph/0609075.

[40] E. Accomando et al., "Workshop on CP studies and non-standard Higgs physics", (2006). arXiv:hep-ph/0608079.

[41] R. M. Godbole, D. J. Miller, and M. M. Mühlleitner, "Aspects of CP violation in the HZZ coupling at the LHC", *JHEP* **12** (2007) 031, doi:10.1088/1126-6708/2007/12/031, arXiv:0708.0458.

[42] K. Hagiwara, Q. Li, and K. Mawatari, "Jet angular correlation in vector-boson fusion processes at hadron colliders", *JHEP* **07** (2009) 101, doi:10.1088/1126-6708/2009/07/101, arXiv:0905.4314.

[43] Y. Gao et al., "Spin determination of single-produced resonances at hadron colliders", *Phys. Rev. D* **81** (2010) 075022, doi:10.1103/PhysRevD.81.075022, arXiv:1001.3396.

[44] A. De Rújula et al., "Higgs look-alikes at the LHC", *Phys. Rev. D* **82** (2010) 013003, doi:10.1103/PhysRevD.82.013003, arXiv:1001.5300.

[45] N. D. Christensen, T. Han, and Y. Li, "Testing CP Violation in ZZH Interactions at the LHC", *Phys. Lett. B* **693** (2010) 28, doi:10.1016/j.physletb.2010.08.008, arXiv:1005.5393.

[46] J. S. Gainer, K. Kumar, I. Low, and R. Vega-Morales, "Improving the sensitivity of Higgs boson searches in the golden channel", *JHEP* **11** (2011) 027, doi:10.1007/JHEP11(2011)027, arXiv:1108.2274.

[47] S. Bolognesi et al., "Spin and parity of a single-produced resonance at the LHC", *Phys. Rev. D* **86** (2012) 095031, doi:10.1103/PhysRevD.86.095031, arXiv:1208.4018.

[48] J. Ellis, D. S. Hwang, V. Sanz, and T. You, "A fast track towards the 'Higgs' spin and parity", *JHEP* **11** (2012) 134, doi:10.1007/JHEP11(2012)134, arXiv:1208.6002.

[49] Y. Chen, N. Tran, and R. Vega-Morales, "Scrutinizing the Higgs signal and background in the $2e2\mu$ golden channel", *JHEP* **01** (2013) 182, doi:10.1007/JHEP01(2013)182, arXiv:1211.1959.

[50] J. S. Gainer et al., "Geolocating the Higgs boson candidate at the LHC", *Phys. Rev. Lett.* **111** (2013) 041801, doi:10.1103/PhysRevLett.111.041801, arXiv:1304.4936.

[51] P. Artoisenet et al., "A framework for Higgs characterisation", *JHEP* **11** (2013) 043, doi:10.1007/JHEP11(2013)043, arXiv:1306.6464.

[52] I. Anderson et al., "Constraining anomalous HVV interactions at proton and lepton colliders", *Phys. Rev. D* **89** (2014) 035007, doi:10.1103/PhysRevD.89.035007, arXiv:1309.4819.

[53] M. Chen et al., "Role of interference in unraveling the ZZ couplings of the newly discovered boson at the LHC", *Phys. Rev. D* **89** (2014) 034002, doi:10.1103/PhysRevD.89.034002, arXiv:1310.1397.

[54] Y. Chen and R. Vega-Morales, "Extracting Effective Higgs Couplings in the Golden Channel", *JHEP* **04** (2014) 057, doi:10.1007/JHEP04(2014)057, arXiv:1310.2893.

[55] J. S. Gainer et al., "Beyond geolocating: Constraining higher dimensional operators in $H \to 4\ell$ with off-shell production and more", *Phys. Rev. D* **91** (2015) 035011, doi:10.1103/PhysRevD.91.035011, arXiv:1403.4951.

[56] M. Gonzalez-Alonso, A. Greljo, G. Isidori, and D. Marzocca, "Pseudo-observables in Higgs decays", *Eur. Phys. J.* **C75** (2015) 128, doi:10.1140/epjc/s10052-015-3345-5, arXiv:1412.6038.

[57] M. J. Dolan, P. Harris, M. Jankowiak, and M. Spannowsky, "Constraining CP-violating Higgs sectors at the LHC using gluon fusion", *Phys. Rev. D* **90** (2014) 073008, doi:10.1103/PhysRevD.90.073008, arXiv:1406.3322.

[58] F. Demartin et al., "Higgs characterisation at NLO in QCD: CP properties of the top-quark Yukawa interaction", *Eur. Phys. J. C* **74** (2014) 3065, doi:10.1140/epjc/s10052-014-3065-2, arXiv:1407.5089.

[59] Y. Chen, R. Harnik, and R. Vega-Morales, "Probing the Higgs Couplings to Photons in $H \to 4\ell$ at the LHC", *Phys. Rev. Lett.* **113** (2014), no. 19, 191801, doi:10.1103/PhysRevLett.113.191801, arXiv:1404.1336.

[60] M. R. Buckley and D. Goncalves, "Boosting the Direct CP Measurement of the Higgs-Top Coupling", *Phys. Rev. Lett.* **116** (2016) 091801, doi:10.1103/PhysRevLett.116.091801, arXiv:1507.07926.

[61] A. Greljo, G. Isidori, J. M. Lindert, and D. Marzocca, "Pseudo-observables in electroweak Higgs production", *Eur. Phys. J. C* **76** (2016) 158, doi:10.1140/epjc/s10052-016-4000-5, arXiv:1512.06135.

[62] A. V. Gritsan, R. Röntsch, M. Schulze, and M. Xiao, "Constraining anomalous Higgs boson couplings to the heavy flavor fermions using matrix element techniques", *Phys. Rev.* **D94** (2016) 055023, doi:10.1103/PhysRevD.94.055023, arXiv:1606.03107.

[63] LHC Higgs Cross Section Working Group Collaboration, "Handbook of LHC Higgs Cross Sections: 4. Deciphering the Nature of the Higgs Sector", doi:10.23731/CYRM-2017-002, arXiv:1610.07922.

[64] C. Hartmann and M. Trott, "Higgs Decay to Two Photons at One Loop in the Standard Model Effective Field Theory", *Phys. Rev. Lett.* **115** (2015), no. 19, 191801, doi:10.1103/PhysRevLett.115.191801, arXiv:1507.03568.

[65] S. Dawson and P. P. Giardino, "Higgs decays to ZZ and $Z\gamma$ in the standard model effective field theory: An NLO analysis", *Phys. Rev.* **D97** (2018), no. 9, 093003, doi:10.1103/PhysRevD.97.093003, arXiv:1801.01136.

[66] A. Dedes et al., "The decay $h \to \gamma\gamma$ in the Standard-Model Effective Field Theory", *JHEP* **08** (2018) 103, doi:10.1007/JHEP08(2018)103, arXiv:1805.00302.

[67] S. Dawson and P. P. Giardino, "Electroweak corrections to Higgs boson decays to $\gamma\gamma$ and W^+W^- in standard model EFT", *Phys. Rev.* **D98** (2018), no. 9, 095005, doi:10.1103/PhysRevD.98.095005, arXiv:1807.11504.

[68] I. Brivio, T. Corbett, and M. Trott, "The Higgs width in the SMEFT", *JHEP* **10** (2019) 056,

doi:10.1007/JHEP10(2019)056, arXiv:1906.06949.
[69] A. V. Gritsan et al., "New features in the JHU generator framework: constraining Higgs boson properties from on-shell and off-shell production", *Phys. Rev. D* **102** (2020), no. 5, 056022, doi:10.1103/PhysRevD.102.056022, arXiv:2002.09888.
[70] T. Martini, R.-Q. Pan, M. Schulze, and M. Xiao, "Probing the CP structure of the top quark Yukawa coupling: Loop sensitivity versus on-shell sensitivity", *Phys. Rev. D* **104** (2021), no. 5, 055045, doi:10.1103/PhysRevD.104.055045, arXiv:2104.04277.
[71] J. Davis et al., "Constraining anomalous Higgs boson couplings to virtual photons", *Phys. Rev. D* **105** (2022), no. 9, 096027, doi:10.1103/PhysRevD.105.096027, arXiv:2109.13363.
[72] R. K. Barman, D. Gonçalves, and F. Kling, "Machine learning the Higgs boson-top quark CP phase", *Phys. Rev. D* **105** (2022), no. 3, 035023, doi:10.1103/PhysRevD.105.035023, arXiv:2110.07635.
[73] R. K. Barman et al., "Directly Probing the CP-structure of the Higgs-Top Yukawa at HL-LHC and Future Colliders", in *2022 Snowmass Summer Study*. 3, 2022. arXiv:2203.08127.
[74] ATLAS Collaboration, "Observation of a new particle in the search for the Standard Model Higgs boson with the ATLAS detector at the LHC", *Phys. Lett.* **B716** (2012) 1–29, doi:10.1016/j.physletb.2012.08.020, arXiv:1207.7214.
[75] CMS Collaboration, "Observation of a new boson at a mass of 125 GeV with the CMS experiment at the LHC", *Phys. Lett.* **B716** (2012) 30–61, doi:10.1016/j.physletb.2012.08.021, arXiv:1207.7235.
[76] S. Dawson et al., "Working Group Report: Higgs Boson", in *Community Summer Study 2013: Snowmass on the Mississippi*. 10, 2013. arXiv:1310.8361.
[77] "LHC Higgs Working Group",. https://twiki.cern.ch/twiki/bin/view/LHCPhysics/LHCHWG.
[78] "LHC EFT Working Group",. https://lpcc.web.cern.ch/lhc-eft-wg.
[79] J. de Blas et al., "Higgs Boson Studies at Future Particle Colliders", *JHEP* **01** (2020) 139, doi:10.1007/JHEP01(2020)139, arXiv:1905.03764.
[80] S. Dawson et al., "Report of the Topical Group on Higgs Physics for Snowmass 2021: The Case for Precision Higgs Physics", in *2022 Snowmass Summer Study*. 9, 2022. arXiv:2209.07510.
[81] F. Bishara et al., "Probing CP Violation in $h \to \gamma\gamma$ with Converted Photons", *JHEP* **04** (2014) 084, doi:10.1007/JHEP04(2014)084, arXiv:1312.2955.
[82] B. Grzadkowski and J. F. Gunion, "Using back scattered laser beams to detect CP violation in the neutral Higgs sector", *Phys. Lett. B* **294** (1992) 361–368, doi:10.1016/0370-2693(92)91534-G, arXiv:hep-ph/9206262.
[83] M. Kramer, J. H. Kuhn, M. L. Stong, and P. M. Zerwas, "Prospects of measuring the parity of Higgs particles", *Z. Phys. C* **64** (1994) 21–30, doi:10.1007/BF01557231, arXiv:hep-ph/9404280.
[84] J. F. Gunion and J. G. Kelly, "Determining the CP eigenvalues of the neutral Higgs bosons of the minimal supersymmetric model in gamma gamma collisions", *Phys. Lett. B* **333** (1994) 110–117, doi:10.1016/0370-2693(94)91015-4, arXiv:hep-ph/9404343.
[85] D. M. Asner, J. B. Gronberg, and J. F. Gunion, "Detecting and studying Higgs bosons at a photon-photon collider", *Phys. Rev. D* **67** (2003) 035009, doi:10.1103/PhysRevD.67.035009, arXiv:hep-ph/0110320.
[86] W. Chou et al., "HFiTT - Higgs Factory in Tevatron Tunnel", arXiv:1305.5202.
[87] B. Grzadkowski, J. F. Gunion, and J. Pliszka, "How valuable is polarization at a muon collider? A Test case: Determining the CP nature of a Higgs boson", *Nucl. Phys. B* **583** (2000) 49–75, doi:10.1016/S0550-3213(00)00229-7, arXiv:hep-ph/0003091.
[88] CMS Collaboration, "Supplemental materials: Constraints on anomalous Higgs boson couplings to vector bosons and fermions f rom the production of Higgs bosons using the $\tau\tau$ final state",. http://cms-results.web.cern.ch/cms-results/public-results/publications/HIG-20-007/.
[89] Y. Chen, A. Falkowski, I. Low, and R. Vega-Morales, "New Observables for CP Violation in Higgs Decays", *Phys. Rev. D* **90** (2014), no. 11, 113006, doi:10.1103/PhysRevD.90.113006, arXiv:1405.6723.
[90] M. Cepeda et al., "Higgs Physics at the HL-LHC and HE-LHC", *CERN Yellow Rep. Monogr.* **7** (2019) 221–584, doi:10.23731/CYRM-2019-007.221, arXiv:1902.00134.
[91] Particle Data Group Collaboration, "Review of Particle Physics", *PTEP* **2020** (2020), no. 8, 083C01, doi:10.1093/ptep/ptaa104.
[92] G. Mahlon and S. J. Parke, "Spin Correlation Effects in Top Quark Pair Production at the LHC", *Phys. Rev. D* **81** (2010) 074024, doi:10.1103/PhysRevD.81.074024, arXiv:1001.3422.
[93] D. Gonçalves, K. Kong, and J. H. Kim, "Probing the top-Higgs Yukawa CP structure in dileptonic $t\bar{t}h$ with M_2-assisted reconstruction", *JHEP* **06** (2018) 079, doi:10.1007/JHEP06(2018)079, arXiv:1804.05874.
[94] D. Gonçalves, J. H. Kim, K. Kong, and Y. Wu, "Direct Higgs-top CP-phase measurement with $t\bar{t}h$ at the 14 TeV LHC and 100 TeV FCC", *JHEP* **01** (2022) 158, doi:10.1007/JHEP01(2022)158, arXiv:2108.01083.
[95] W. Bernreuther and Z.-G. Si, "Distributions and correlations for top quark pair production and decay at the Tevatron and LHC.", *Nucl. Phys. B* **837** (2010) 90–121, doi:10.1016/j.nuclphysb.2010.05.001, arXiv:1003.3926.
[96] H. Bahl et al., "Indirect $\mathcal{CP}$ probes of the Higgs-top-quark interaction: current LHC constraints and future opportunities", *JHEP* **11** (2020) 127, doi:10.1007/JHEP11(2020)127, arXiv:2007.08542.
[97] H. Bahl and S. Brass, "Constraining $\mathcal{CP}$-violation in the Higgs-top-quark interaction using machine-learning-based inference", *JHEP* **03** (2022) 017, doi:10.1007/JHEP03(2022)017, arXiv:2110.10177.
[98] S. Berge, W. Bernreuther, B. Niepelt, and H. Spiesberger, "How to pin down the CP quantum numbers of a Higgs boson in its tau decays at the LHC", *Phys. Rev. D* **84** (2011) 116003, doi:10.1103/PhysRevD.84.116003, arXiv:1108.0670.

[99] R. Harnik et al., "Measuring CP Violation in $h \to \tau^+\tau^-$ at Colliders", *Phys. Rev. D* **88** (2013), no. 7, 076009, doi:10.1103/PhysRevD.88.076009, arXiv:1308.1094.

[100] A. Askew et al., "Prospect for measuring the CP phase in the $h\tau\tau$ coupling at the LHC", *Phys. Rev. D* **91** (2015), no. 7, 075014, doi:10.1103/PhysRevD.91.075014, arXiv:1501.03156.

[101] ATLAS Collaboration, "Probing the CP nature of the Higgs boson coupling to τ leptons at HL-LHC",. https://cds.cern.ch/record/2665667.

[102] CMS Collaboration, "Supplemental materials: Analysis of the CP structure of the Yukawa coupling between the Higgs boson and τ leptons in proton-proton collisions at $\sqrt{s} = 13$ TeV",. http://cms-results.web.cern.ch/cms-results/public-results/publications/HIG-20-006/.

[103] ECFA/DESY LC Physics Working Group Collaboration, "TESLA: The Superconducting electron positron linear collider with an integrated x-ray laser laboratory. Technical design report. Part 3. Physics at an e+ e- linear collider", arXiv:hep-ph/0106315.

[104] Q. Sha et al., "Probing Higgs CP properties at the CEPC", arXiv:2203.11707.

[105] N. Craig, J. Gu, Z. Liu, and K. Wang, "Beyond Higgs Couplings: Probing the Higgs with Angular Observables at Future e^+ $e^?$ Colliders", *JHEP* **03** (2016) 050, doi:10.1007/JHEP03(2016)050, arXiv:1512.06877.

[106] M. Beneke, D. Boito, and Y.-M. Wang, "Anomalous Higgs couplings in angular asymmetries of $H \to Z\ell^+\ell^-$ and e^+ $e^- \to HZ$", *JHEP* **11** (2014) 028, doi:10.1007/JHEP11(2014)028, arXiv:1406.1361.

[107] T. Ogawa, J. Tian, and K. Fujii, "Sensitivity to anomalous ZZH couplings at the ILC", *PoS* **EPS-HEP2017** (2017) 322, doi:10.22323/1.314.0322, arXiv:1712.09772.

[108] I. Božović-Jelisavucić, N. Vukausinović, and D. Jeans, "Measuring the CP properties of the Higgs sector at electron-positron colliders", in *2022 Snowmass Summer Study*. 3, 2022. arXiv:2203.06819.

[109] N. Vukasinovic, "Determination of CPV Higgs mixing angle in ZZ-fusion at 1.4 TeV CLIC",. https://agenda.infn.it/event/28874/contributions/170893/attachments/94395/129150/ICHEP2022_nvukasinovic_final.pdf.

[110] T. Price, P. Roloff, J. Strube, and T. Tanabe, "Full simulation study of the top Yukawa coupling at the ILC at $\sqrt{s} = 1$ TeV", *Eur. Phys. J. C* **75** (2015), no. 7, 309, doi:10.1140/epjc/s10052-015-3532-4, arXiv:1409.7157.

[111] CLICdp Collaboration, "Top-Quark Physics at the CLIC Electron-Positron Linear Collider", *JHEP* **11** (2019) 003, doi:10.1007/JHEP11(2019)003, arXiv:1807.02441.

[112] Y. Zhang, "Prospects for Precision Measurements of the Top-Yukawa Coupling and CP Violation in ttH Production at the CLIC e^+e^- Collider",. https://cds.cern.ch/record/2747738/files/CERN-THESIS-2020-232.pdf.

[113] K. Desch, A. Imhof, Z. Was, and M. Worek, "Probing the CP nature of the Higgs boson at linear colliders with tau spin correlations: The Case of mixed scalar - pseudoscalar couplings", *Phys. Lett. B* **579** (2004) 157–164, doi:10.1016/j.physletb.2003.10.074, arXiv:hep-ph/0307331.

[114] S. Berge, W. Bernreuther, and H. Spiesberger, "Determination of the CP parity of Higgs bosons in their tau decay channels at the ILC", in *International Workshop on Future Linear Colliders (LCWS11)*, pp. 248–257. DESY, Hamburg, 8, 2012. arXiv:1208.1507.

[115] S. Berge, W. Bernreuther, and H. Spiesberger, "Higgs CP properties using the τ decay modes at the ILC", *Phys. Lett. B* **727** (2013) 488–495, doi:10.1016/j.physletb.2013.11.006, arXiv:1308.2674.

[116] D. Jeans and G. W. Wilson, "Measuring the CP state of tau lepton pairs from Higgs decay at the ILC", *Phys. Rev. D* **98** (2018), no. 1, 013007, doi:10.1103/PhysRevD.98.013007, arXiv:1804.01241.

[117] LHeC, FCC-he Study Group Collaboration, "The Large Hadron–Electron Collider at the HL-LHC", *J. Phys. G* **48** (2021), no. 11, 110501, doi:10.1088/1361-6471/abf3ba, arXiv:2007.14491.

[118] S. S. Biswal, R. M. Godbole, B. Mellado, and S. Raychaudhuri, "Azimuthal Angle Probe of Anomalous HWW Couplings at a High Energy ep Collider", *Phys. Rev. Lett.* **109** (2012) 261801, doi:10.1103/PhysRevLett.109.261801, arXiv:1203.6285.

[119] I. T. Cakir, O. Cakir, A. Senol, and A. T. Tasci, "Probing Anomalous HZZ Couplings at the LHeC", *Mod. Phys. Lett. A* **28** (2013), no. 31, 1350142, doi:10.1142/S0217732313501423, arXiv:1304.3616.

[120] P. Sharma and A. Shivaji, "Probing non-standard $HVV(V = W, Z)$ couplings in single Higgs production at future electron-proton collider", arXiv:2207.03862.

[121] B. Coleppa, M. Kumar, S. Kumar, and B. Mellado, "Measuring CP nature of top-Higgs couplings at the future Large Hadron electron collider", *Phys. Lett. B* **770** (2017) 335–341, doi:10.1016/j.physletb.2017.05.006, arXiv:1702.03426.

[122] R. Alarcon et al., "Electric dipole moments and the search for new physics", in *2022 Snowmass Summer Study*. 3, 2022. arXiv:2203.08103.

[123] M. Pospelov and A. Ritz, "Electric dipole moments as probes of new physics", *Annals Phys.* **318** (2005) 119–169, doi:10.1016/j.aop.2005.04.002, arXiv:hep-ph/0504231.

[124] Y. Li, S. Profumo, and M. Ramsey-Musolf, "A Comprehensive Analysis of Electric Dipole Moment Constraints on CP-violating Phases in the MSSM", *JHEP* **08** (2010) 062, doi:10.1007/JHEP08(2010)062, arXiv:1006.1440.

[125] V. Cirigliano, W. Dekens, J. de Vries, and E. Mereghetti, "Constraining the top-Higgs sector of the Standard Model Effective Field Theory", *Phys. Rev. D* **94** (2016), no. 3, 034031, doi:10.1103/PhysRevD.94.034031, arXiv:1605.04311.

[126] V. Cirigliano et al., "CP Violation in Higgs-Gauge Interactions: From Tabletop Experiments to the LHC", *Phys. Rev. Lett.* **123** (2019), no. 5, 051801, doi:10.1103/PhysRevLett.123.051801, arXiv:1903.03625.

[127] H. Bahl et al., "Constraining the CP structure of Higgs-fermion couplings with a global LHC fit, the electron EDM and baryogenesis", arXiv:2202.11753.

[128] ACME Collaboration, "Improved limit on the electric dipole moment of the electron", *Nature* **562** (2018), no. 7727, 355–360, doi:10.1038/s41586-018-0599-8.

[129] C. Abel et al., "Measurement of the Permanent Electric Dipole Moment of the Neutron", *Phys. Rev. Lett.* **124** (2020), no. 8, 081803, doi:10.1103/PhysRevLett.124.081803, arXiv:2001.11966.

[130] B. Graner, Y. Chen, E. G. Lindahl, and B. R. Heckel, "Reduced Limit on the Permanent Electric Dipole Moment of Hg199", *Phys. Rev. Lett.* **116** (2016), no. 16, 161601, doi:10.1103/PhysRevLett.116.161601, arXiv:1601.04339. [Erratum: Phys.Rev.Lett. 119, 119901 (2017)].

[131] J. Alexander et al., "The storage ring proton EDM experiment", arXiv:2205.00830.

[132] J. Brod, U. Haisch, and J. Zupan, "Constraints on CP-violating Higgs couplings to the third generation", *JHEP* **11** (2013) 180, doi:10.1007/JHEP11(2013)180, arXiv:1310.1385.

[133] J. Brod, J. M. Cornell, D. Skodras, and E. Stamou, "Global Constraints on Yukawa Operators in the Standard Model Effective Theory", arXiv:2203.03736.

[134] Y. T. Chien et al., "Direct and indirect constraints on CP-violating Higgs-quark and Higgs-gluon interactions", *JHEP* **02** (2016) 011, doi:10.1007/JHEP02(2016)011, arXiv:1510.00725.

[135] W. Dekens and J. de Vries, "Renormalization Group Running of Dimension-Six Sources of Parity and Time-Reversal Violation", *JHEP* **05** (2013) 149, doi:10.1007/JHEP05(2013)149, arXiv:1303.3156.

[136] J. Fan and M. Reece, "Probing Charged Matter Through Higgs Diphoton Decay, Gamma Ray Lines, and EDMs", *JHEP* **06** (2013) 004, doi:10.1007/JHEP06(2013)004, arXiv:1301.2597.

[137] A. De Rujula, M. B. Gavela, O. Pene, and F. J. Vegas, "Signets of CP violation", *Nucl. Phys. B* **357** (1991) 311–356, doi:10.1016/0550-3213(91)90472-A.

[138] S. M. Barr and A. Zee, "Electric Dipole Moment of the Electron and of the Neutron", *Phys. Rev. Lett.* **65** (1990) 21–24, doi:10.1103/PhysRevLett.65.21.

[139] W. Buchmuller and D. Wyler, "Effective Lagrangian analysis of new interactions and flavor conservation", *Nucl. Phys. B* **268** (1986) 621, doi:10.1016/0550-3213(86)90262-2.

[140] B. Grzadkowski, M. Iskrzynski, M. Misiak, and J. Rosiek, "Dimension-Six Terms in the Standard Model Lagrangian", *JHEP* **10** (2010) 085, doi:10.1007/JHEP10(2010)085, arXiv:1008.4884.

[141] S. Alioli, W. Dekens, M. Girard, and E. Mereghetti, "NLO QCD corrections to SM-EFT dilepton and electroweak Higgs boson production, matched to parton shower in POWHEG", *JHEP* **08** (2018) 205, doi:10.1007/JHEP08(2018)205, arXiv:1804.07407.

[142] J. Engel, M. J. Ramsey-Musolf, and U. van Kolck, "Electric Dipole Moments of Nucleons, Nuclei, and Atoms: The Standard Model and Beyond", *Prog. Part. Nucl. Phys.* **71** (2013) 21–74, doi:10.1016/j.ppnp.2013.03.003, arXiv:1303.2371.

[143] T. Chupp, P. Fierlinger, M. Ramsey-Musolf, and J. Singh, "Electric dipole moments of atoms, molecules, nuclei, and particles", *Rev. Mod. Phys.* **91** (2019), no. 1, 015001, doi:10.1103/RevModPhys.91.015001, arXiv:1710.02504.